FEATURE ARTICLE

Photosynthetic Light-Harvesting: Reconciling Dynamics and Structure of Purple Bacterial LH2 Reveals Function of Photosynthetic Unit

Villy Sundström*,† and Tõnu Pullerits‡

Department of Chemical Physics, Chemical Center, Lund University, P.O. Box 124, 221 00 Lund, Sweden

Rienk van Grondelle§

Department of Physics and Astronomy, Vrije Universiteit, De Boelelaan 1081, 1081 HV Amsterdam, The Netherlands

Received: September 15, 1998; In Final Form: December 18, 1998

Great progress in the study of structure and dynamics of photosynthetic light-harvesting pigment−protein complexes has recently resulted in detailed understanding of the light-harvesting and light-conversion processes of photosynthesis. We review and discuss recent results on the elementary excitation transfer dynamics of the purple bacterial LH2 peripheral complex. When combining the information from the two LH2 structures that are now available with the experimental results obtained from steady-state spectroscopy, a variety of ultrafast techniques and computer simulations, a detailed understanding of the LH2 function is obtained. Dynamics relevant to the complete photosynthetic unit (PSU = LH2 + LH1 core + reaction center), as well as models of the PSU obtained on the basis of the LH2 structure, allow us to suggest how the characteristic structural features of LH2 and LH1 have been designed to optimize the overall light-harvesting and trapping process in the PSU.

1. Introduction

The light-driven reactions of photosynthesis are the means by which nature converts solar energy into a stable electrochemical potential, which eventually is stored as chemical energy through a series of dark reactions. The light reactions occur in two closely coupled pigment systems: light energy is absorbed by a network of so-called antenna pigments bound to proteins and the excitation energy is very efficiently transported to the photochemical reaction center (RC) where the energy is converted into a stable transmembrane charge separation through a sequence of electron-transfer reactions.[1−4] Time-resolved picosecond measurements showed that this conversion process is typically finished within ∼100 ps, explaining the high overall quantum yield (95%) of the process, known already in the early days of photosynthesis research.[5] In the photosynthetic purple bacteria to be discussed in this paper, the light-harvesting antenna generally consists of a core antenna, LH1, which for the bacteriochlorophyll (BChl) *a* containing species absorbs around 870−880 nm, while BChl *b* containing species exhibit major absorption around 1000 nm. An electron microscopy visualization of the photosynthetic membrane of the BChl *b* containing species *Rhodopseudomonas (Rps.) viridis* by Miller[6] showed for the first time how LH1 is arranged as a circle around the RC; the diameter of this RC-LH1 core was about 10−11 nm. In species with LH1 as the single antenna, the RC-LH1 network forms a continuous, sometimes quasi-crystalline domain, in which ultrafast energy transfer occurs. In many BChl *a* containing species such as *Rhodobacter (Rb.) sphaeroides*, *Rhodopseudomonas (Rps.) acidophila*, and *Rhodospirillum (Rs.) molischianum* a second light-harvesting complex occurs, LH2, in general with major absorption at 800 and 850 nm, although LH2s with other absorption maxima occur (830 nm, 820 nm), depending among others on the degree of hydrogen bonding between the pigment and the protein.[7,8] It is generally believed that LH2 is organized peripheral to the RC-LH1 core, but its precise arrangement is unknown and may be rather disordered.

Both LH1 and LH2 have been studied extensively with biochemical techniques.[9] The individual light-harvesting complexes were purified, their protein composition analyzed and, for *Rhodopseudomonas (Rps.) capsulatus* and later *Rb. sphaeroides*, molecular genetics were developed (for a review, see ref 10). Following the large scale purification procedures, attempts to crystallize LH1 and LH2 were very much stimulated by the success of Michel and Deisenhofer with the bacterial reaction center.[11] Largely due to the work of Zuber and co-workers, it has been established that the elementary building block of LH1 and LH2 is a pair of small polypeptides, called α and *β*, and both contain a single transmembrane helix as the major structural element. Both α and *β* bind a single BChl molecule at a conserved histidine residue, positioned in the transmembrane helix, while in the case of LH2 the *β*-polypeptide binds a second

† E-mail: villy.sundstrom@chemphys.lu.se.
‡ E-mail: tonu.pullerits@chemphys.lu.se. Fax: +46 46 2224119.
§ E-mail: rienk@nat.vu.nl.

10.1021/jp983722+ CCC: $18.00
Published on Web 03/17/1999

BChl. The $\alpha\beta$-heterodimers arrange themselves in circular structures that make up LH1 and LH2.[9,12]

Earlier spectroscopic research using polarized light resulted in a detailed picture of how the BChl *a* molecules in LH2 and LH1 were organized. For LH2, a model was proposed by Kramer and co-workers[13] that positioned the B850 BChls in a square, determined by the conserved histidine residues and parallel to the plane of the membrane. The B850s (like the B870s in LH1) had their Q_y transitions in the plane of the membrane, while the Q_x transitions were perpendicular to it. The excitonic interactions between neighboring B850s were sufficiently strong to generate part of the red shift from about 800 nm for protein-bound monomeric BChl to the in vivo absorption around 850 nm. In contrast, the B800s were organized with their macrocycles parallel to the plane of the membrane and the distance between the B850 and B800 plane was estimated to be about 1.5−1.9 nm.[13,14] The model allowed fast energy transfer to occur among the B850s and the B800s, while the B800 → B850 energy transfer was estimated to be in the few picosecond range, consistent with the measured B800 fluorescence quantum yield. The carotenoids were positioned in such a way as to comply with the observed efficient energy transfer to the B800 and B850 BChls (in fact the observed energy transfer efficiency from carotenoid to BChl in LH2 of *Rb. sphaeroides* is >95%; for other LH2s, smaller numbers were reported (see below). From a variety of theoretical considerations, mainly exchange interactions between the carotenoids and the BChls were held responsible, implying van der Waals contacts between them.[15]

In the 1980s a variety of experiments were initiated applying short (picosecond) laser pulses. To explain the very efficient annihilation of excitations in LH1 and LH2, single-site excited-state lifetimes of much less than a picosecond had to be assumed.[16] Low intensity, high repetition rate pulses were applied later, and either the spontaneous emission[17] or the time-resolved transmission[18] was detected. Although the time-resolution of these experiments was not sufficient to resolve the ultrafast kinetics, upper limits for many of the essential steps became available, to be confirmed later by experiments with shorter pulses (see below).

The B800 → 850 energy transfer time in LH2 of *Rb. sphaeroides* was found to be about 1 ps using "long" ~10 ps pulses;[18−21] later a time constant of about 0.7 ps at room temperature was firmly established.[22,23] The B800 → B850 energy transfer rate is weakly temperature dependent; at 77 K the time constant was found to be about 1 ps[24] and it slows down further at 4 K.[25−27] For other LH2s similar time constants were obtained.[28−35] The detailed discussion of this transfer step is in section 6. The B800 → B800 energy transfer time (see section 5) was more difficult to establish, a variety of studies put it in the 0.3−1 ps range for LH2 of *Rb. sphaeroides* and *Rps. acidophila*.[23,36] For *Rs. molischianum* the intra-B800 energy transfer rate is most likely slower.[37] Energy transfer in the B850 ring must be very fast. From several recent studies employing sub-100-fs Ti:Sapphire laser pulses, a general consensus has emerged that the single site excited-state lifetime for B850 is in the 100 fs range (see section 7).

The early time-resolved studies on carotenoid to BChl energy transfer in LH2 also implicated the involvement of the forbidden 2^1A_g state mainly via an exchange process. More recent studies using sub-100-fs laser pulses ascribe an essential part of the energy transfer from carotenoid to BChl to the short-lived but strongly dipole-allowed ^1B_u state of the carotenoid (see section 4).

A multitude of time constants was reported for the LH2→LH1 energy transfer, ranging between 3 and 40 ps.[21,38] More recently it was established that the dominant time constant for this step is in the 3−5 ps range.[39,40] Finally, the early experiments firmly established the time required for the excitation to be trapped from the LH1 core by the active reaction center to be about 50−60 ps for many species.[17,18,41,42] In fact the rate-limiting step in this reaction is not the intra-LH2, the intra-LH1, or the LH2→LH1 energy transfer, but the transfer from any of the LH1 sites to the special pair of the RC. It was concluded that this step must occur over a relatively large distance of about 3−4 nm.[43,44]

A major breakthrough in our understanding of the organization of the bacterial light-harvesting antenna and consequently of the process itself came with the discovery of the structure of the LH2 complex of *Rps. acidophila* by Cogdell and co-workers in 1995,[45] followed by the structure of *Rs. molischianum* by Michel and Schulten and co-workers in 1996.[46] These structures revealed the 9- and 8-fold symmetric rings of $\alpha\beta$-heterodimers for *Rps. acidophila* and *Rs. molischianum*, respectively. On the basis of a low-resolution electron density map and the analogy between LH2 and LH1, it is now generally believed that LH1 is a 16-fold symmetric ring of $\alpha\beta$-heterodimers, with the RC in its center.[47] These structures have stimulated a large body of experimental and theoretical work on photosynthetic light harvesting. In this feature article we wish to discuss the remarkable progress that has been made in our understanding of the energy transfer dynamics and spectroscopy of LH2. We will highlight shortly some relevant aspects of the LH2 structure, discuss some aspects of the theory relevant for the spectroscopy and energy transfer dynamics of circular aggregates, and describe the various energy transfer events that occur in LH2: carotenoid to B800 and B850, B800 to B800, B800 to B850 and finally the energy transfer dynamics within the B850 ring. We will end the article by an overview of the dynamics of the whole photosynthetic unit and some speculations.

2. Structure of LH2 of *Rhodopseudomonas Acidophila* and *Rhodospirillum Molischianum*

Figure 1 shows a schematic representation of the 2.5 Å LH2 structure of *Rps. acidophila* as obtained by Cogdell and co-workers.[45] The complex is a nonameric circular aggregate of $\alpha\beta$-heterodimers, with each subunit noncovalently binding three BChls and most likely two carotenoids. The aggregate is formed by two concentric rings of helical protein subunits with the α-poplypeptides inside and the βs outside. The B850 ring is formed by the nine pairs of BChls associated with the conserved histidines and is sandwiched between the concentric rings of α- and β-polypeptides. Note that the relative orientation of the BChls alternates, within a subunit there is ring I overlap between the macrocycles, such as in the RC special pair, while between adjacent subunits the overlap is between rings III. The inter- and intrasubunit BChl−BChl center-to-center distances are very similar, about 9 Å; however, due to the fact that the β-B850 is strongly bent, there is more or less continuous electron density within an $\alpha\beta$-subunit, whereas the electron density between BChls on adjacent subunits is discontinuous. The 9 B800s are in a plane about 1.7 nm shifted toward the cytosolic side of the membrane and positioned between the β-helices. The B800−B800 center-to-center distance is about 21.2 Å. A summary of all the relevant distances, dipole−dipole interactions is given in Table 1. In the structure, only one carotenoid is well-resolved and a schematic view of its position relative to the B800 and B850 BChls is given in Figure 2. The rhodopin glucoside

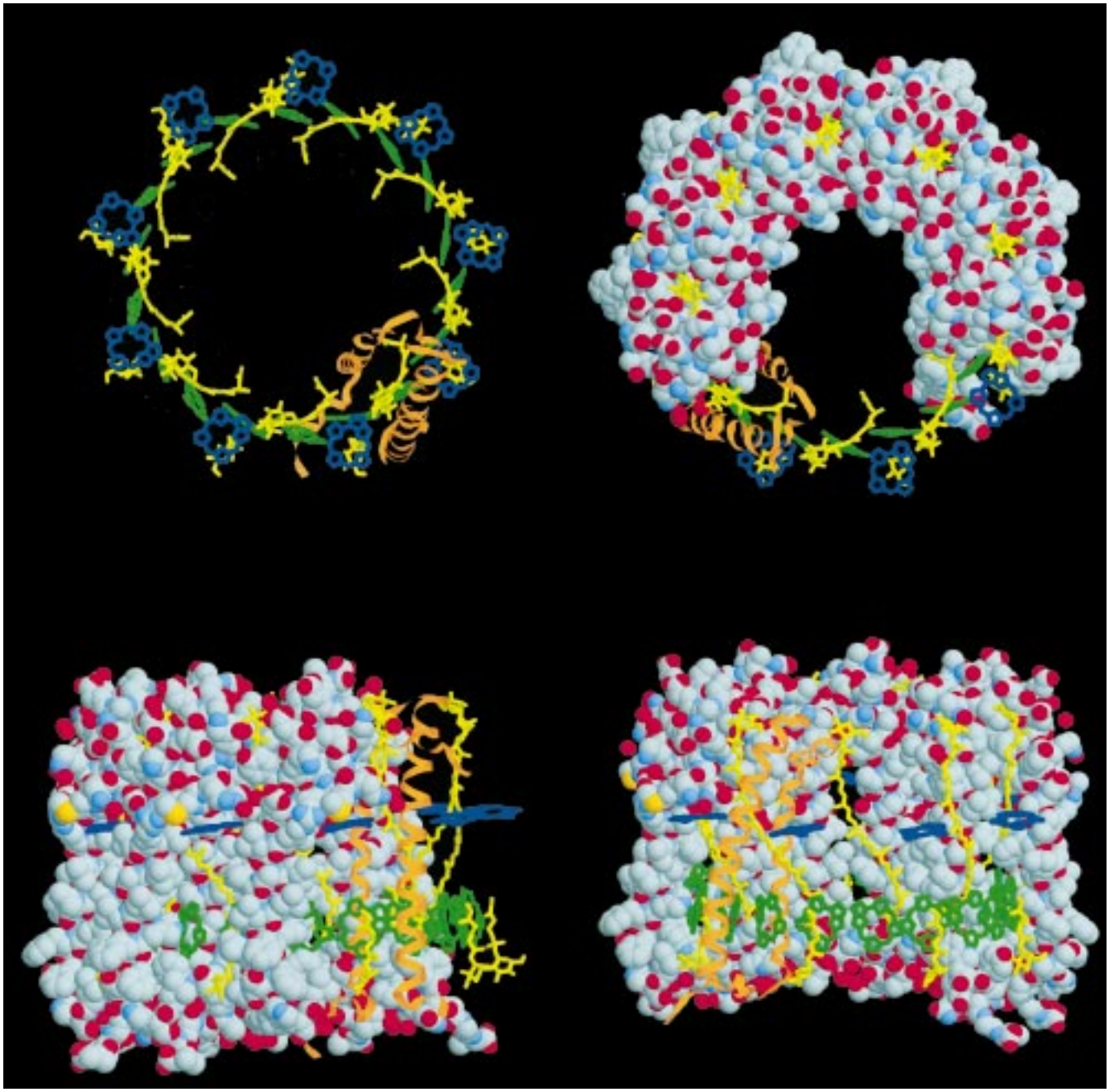

Figure 1. Structure of the LH2 antenna from *Rps. acidophila*. The upper parts are parallel and the lower panels perpendicular to the membrane. In three parts, two-thirds of the LH2 protein is shown via space filled atoms of corresponding van der Waals' radii. One $\alpha\beta$ polypeptide pair is represented via orange ribons. For clarity we show only the porphyrin macrocycles of the Bchl *a* molecules. The B800 Bchl *a* molecules (blue bonds) are parallel to the membrane plane, whereas B850 molecules (green bonds) are perpendicular to the membrane plane. The carotenoid molecules are yellow. We point out that one of the carotenoid molecules is only partly resolved.

molecule transverses the membrane, its polar headgroup is buried in a polar pocket at the cytosolic side of the membrane, it then passes the B800 BChl of the same subunit at close to van der Waals contact, and finally the end of the carotenoid makes close nonbonding contacts with the C(20) and C(27) carbon atoms of the α-B850 pigment in the next subunit. Although the location of the second carotenoid could not be determined from the crystal structure, a detailed analysis suggests that it starts off from the periplasmic side, and then passes the same α-B850 BChl as the first carotenoid, but this time on the outside face of the BChl plane.

The structure of the LH2 complex of *Rs. molischianum* is very closely related to that of LH2 of *Rps. acidophila*. The most conspicious difference is of course that this LH2 is an $\alpha\beta$-octamer with 16 B850 BChls and 8 B800s. It is interesting to note that the octameric structure of LH2 of *Rs. molischianum* was correctly proposed already in an early biochemical study.[48] All relevant distances and dipole−dipole couplings are presented in Table 1. In the structure, one lycopene carotenoid molecule per $\alpha\beta$-subunit is resolved, whose position is very close to that of the structurally resolved carotenoid in LH2 of *Rps. acidophila* shown in Figure 2. One other major difference is that in LH2 of *Rs. molischianum* the plane of the B800s is rotated by about 90° compared to *Rps. acidophila*, resulting in a significantly weaker coupling between the B800 BChls. Less obvious differences include the fact that the central Mg-binding histidine is also making an H-bond with the 9-keto group of the second B850 BChl within the same subunit, very much analogous to

TABLE 1. Comparison of the Structures of LH2s from *Rs. molischianum* and *Rps. acidophila*. For the Dipole−Dipole Interaction Calculation $\mu^2 = 68$ D^2 and $n^2 = 2$ Was Used

	Rs. molischianum octamer	*Rps. acidophila* nonamer
B850		
nearest-neighbor distance in angstroms		
intradimer	9.4	9.5
interdimer	8.7	8.9
dipole−dipole coupling according to (2) in cm^{-1}		
intradimer	339	322
interdimer	336	288
B800		
nearest-neighbor distance in angstroms	22.0	21.3
dipole−dipole coupling according to (2) in cm^{-1}	−14	−22
B800−B850		
nearest-neighbor distance in angstroms	19.1	17.7
four strongest dipole−dipole couplings according to (2) in cm^{-1}	−22.7 15.7 3.8 2.9	25.7 −11.3 6.1 4.8

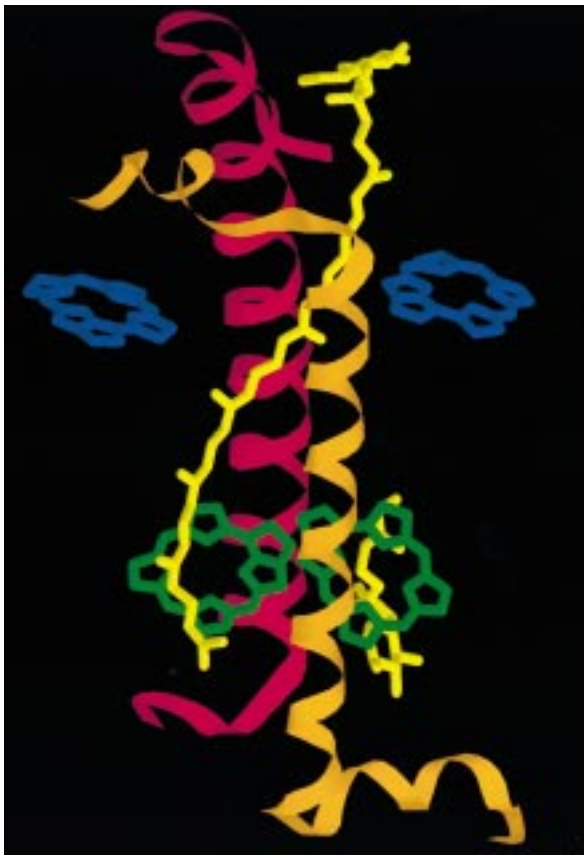

Figure 2. Structure of one $\alpha\beta$ subunit of LH2 of *Rps. acidophila* as seen from inside of the LH2 ring. The color coding of pigments as in Figure 1. Orange and red ribons are α- and β-helices, respectively. To demonstrate the very close approach between a B800 Bchl *a* and a carotenoid molecule we have also shown a B800 molecule (right) of the neighboring subunit.

the situation in LH1 (at least on the basis of Raman and mutagenesis studies[49,50]), and furthermore that the B800 macrocycles are significantly tilted away by about 30° from the membrane plane.

3. Theory for Energy Transfer and Spectroscopy

Excitation transfer in photosynthetic antenna systems has usually been described as an incoherent Förster[51] hopping in a two-dimensional antenna array of pigment molecules.[52−57] It is hard to overestimate the physical insight obtained by this approach. At the same time a number of experimental facts do not fit into this picture, for example, coherent nuclear motions in the antenna systems of photosynthetic purple bacteria[58−60] or the highly structured spectra of so-called Fenna−Matthews−Olson complexes.[61] Particularly the latter case calls for the molecular exciton description[62] where an excitation is coherently delocalized over a number of pigment molecules and the absorption spectrum exhibits a prominent exciton band structure. Time evolution in the exciton picture occurs via phonon induced relaxation between exciton levels. These two descriptions, incoherent hopping and exciton relaxation, are the two qualitatively different limiting cases of the general process of excitation dynamics. What description should be chosen for a particular observation depends on the system properties and the experimental conditions. It may happen that the real situation is somewhere between these two limiting cases, in which case the analyses is particularly challenging. The important factor deciding which processes occurs, is the ratio of the coupling between electronic transitions (V) and the disorder (Δ). The disorder may be either static (spectral inhomogeneity) or dynamic (electron−phonon interaction). The dynamic disorder involves an additional important characteristic: the inverse correlation time of phonon bath.[63] If V/Δ is much less than unity, we are talking about very weak interactions and energy transfer is in the incoherent hopping limit. In the opposite case, if $V/\Delta \gg 1$, the interaction is very strong and the exciton picture is used. In both cases, the transfer rate can be calculated using first-order perturbation theory leading to the Fermi Golden rule. In the hopping description, electronic coupling (V) acts as a perturbation; in exciton picture, electron phonon coupling (dynamic disorder) is the perturbation. The real experimental situation determines which part of the Hamiltonian should be taken as a perturbation and in which basis (excitonic or molecular) to think and work. The two processes (hopping and exciton relaxation) coexist and they are both accounted for in a density matrix formulation of the dynamics.[64,65]

Incoherent Hopping Transfer. The starting point in this approach is an electronic excitation at a single antenna site, which can be a pigment molecule or sometimes an aggregate of a number of molecules (a dimer, etc.). The excited states of the molecules are rather well understood and the dynamics are directly related to the spatial motion of the excitation, which leads to an intuitive visual picture of the process. We do not derive the Förster equation here and refer interested readers to

Förster's original work,[51] or to a recent article by Laible et al.[66] The resulting equation for the pairwise transfer rate can be written as[27]

$$k = 1.18V^2\Theta \tag{1}$$

where k is in ps^{-1}, V is the electronic coupling matrix element between initial and final states in cm^{-1}, and Θ is the overlap integral between the donor emission and acceptor absorption spectra for which the intensity (area) has been normalized to 1 on the cm^{-1} scale. Despite the apparent simplicity, eq 1 has a number of interesting properties. First of all, the dependence of the transfer rate on temperature and energy gap between the molecules is provided via the temperature dependence of the electron vibrational spectra[67] of the molecules involved in the spectral overlap Θ. In direct analogy to the Marcus theory of electron transfer,[68] the excitation transfer rate has an inverted region where the transfer rate decreases if the downhill energy gap increases.[27] Broadening of the spectra with increasing temperature leads to a negative temperature dependence of the transfer rate for moderate downhill energy gaps[27] and warrants the fulfillment of the detailed balance relation between the forward/backward rates.[57,66] Here we point out that, if the donor and acceptor molecules are different, then the energy gap between them is generally not equal to the energy gap between their absorption maxima, but should be taken as the difference in 0−0 transition energies.[69] In Förster theory, V is the dipole−dipole interaction between molecular electronic transition dipole moments:

$$V = 5.04\frac{\mu^2}{R^2 n^2}(\cos\alpha - 3\cos\beta_1\cos\beta_2) \tag{2}$$

where V is in cm^{-1}, μ is the dipole moment in a vacuum in debye ($\mu^2 = 68$ D^2 for BChl a[70]), R is the dipole separation in nm, and n is the refractive index of the medium (usually $n^2 = 2$ is used for proteins), α is the angle between the dipoles, and β_1 and β_2 are the angles between each dipole and the vector connecting them. We have used eq 2 to evaluate the most characteristic interactions in two LH2 structures (see Table 1). Taking the interaction between B800 molecules of *Rps. acidophila* to be 22 cm^{-1} and $\Theta = 0.0035$[27] results in a pairwise transfer time of 0.5 ps, in good agreement with experimental results (see below). Besides the dipole−dipole interaction, the incoherent transfer rate also involves contributions from exchange interaction and higher multipole interactions which were incorporated into the theory by Dexter.[71] Various refinements for interaction calculations have been developed. Here we mention the monopole method[72] and the more recent ab initio transition density cube method.[73] It has been pointed out that short-range excitation transfer rates may be influenced also by interactions mediated by the second-order matrix elements involving charge-transfer configurations of the molecular system.[74] Also higher order superexchange-like terms via nearby chromophores can give a contribution to V. One has to be careful when adding up various terms since different contributions to V may have different signs leading to cancelation. The important point here is that for all these electronic coupling contributions, the nuclear overlap and consequently the spectral overlap integral Θ is the same. Finally we stress that the calculated interactions should be taken as estimates even with the atomic coordinates in hand, and the precise value must still be obtained from experiment.

Having transfer rates, it is easy to write down the master equation describing the excitation dynamics in the photosynthetic unit (PSU) consisting of the antenna and RC:

$$\begin{cases} \dot{p}_i = \sum_{j=1}^{N}(p_j W_{ji} - p_i W_{ij}) - \dfrac{p_i}{\tau_l} - \delta_{1i}\left(\dfrac{p_1}{\tau_{RC}} - \dfrac{p_0}{\tau_{RC}}\right) \\ \dot{p}_0 = \dfrac{p_1}{\tau_{RC}} - p_0\left(\dfrac{\exp(-\Delta E_{RC}/k_B T)}{\tau_{RC}} + \dfrac{1}{\tau_Q}\right) \end{cases} \tag{3}$$

Here p_i is the probability that an excitation is at antenna site i; p_0 denotes the radical pair P^+I^- and p_1 is the excited RC special pair. $N-1$ is the number of antenna sites in a PSU, τ_l is the time of excitation decay due to all losses in the antenna except quenching by the RC, δ_{ij} is the Kronecker symbol, τ_{RC} is the primary charge separation time in the RC and τ_Q is the electron-transfer time to the secondary acceptor Q, ΔE_{RC} is the free energy difference between P*I and P^+I^-, k_B is the Boltzmann constant, and T is the absolute temperature. W_{ij} is the rate of excitation transfer from site i to site j basically given by eq 1. The master eq 3 can be solved by various methods. Usually it is done numerically using the Green's function method, which gives the kinetics of the probability p_i as a sum of N exponentials.[56,57,75] As a result, after performing the ensemble averaging over possible different energetic configurations, one can express the transient absorption and/or fluorescence spectra as a function of excitation and recording wavelengths via distribution of exponential decays ρ[57]

$$I(t,\lambda_{exc},\lambda_{rec}) = \int_0^\infty \rho(\lambda_{exc},\lambda_{rec},\tau)\exp(-t/\tau)\mathrm{d}\tau \tag{4}$$

Excitons. If the interaction V is strong, then the exciton picture is used. The electronic Hamiltonian of a molecular aggregate is expressed as[62]

$$H_{ex} = \sum_i (E + D_i + \Delta_i)|i\rangle\langle i| + \sum_{i,j} V_{ij}|i\rangle\langle j| \equiv \sum_{i,j}\hbar H_{ij}|i\rangle\langle j| \tag{5}$$

where E is the electronic transition energy of the free monomer. D_i is the solvent shift caused by the dispersive interaction of the ith molecule (site) with its specific environment, also the spectral shifts caused by hydrogen bounding is included in this term. D_i is the origin of spectral heterogeneity. Δ_i is a random shift from the average energy $E + D_i$ caused by the stochastic fluctuations in the environment of the ith molecule. Δ_i is the origin of inhomogeneous broadening. V_{ij} is the (dipole−dipole) interaction energy between the ith sites i and jth; $|i\rangle$ and $\langle i|$ are the Dirac ket and bra vectors in which only the ith molecule i is excited.

The Hamiltonian (5) conserves the number of excitations and the eigenstates separate into classes of linear combinations of site states with a fixed number of molecules excited. Correspondingly, also eigenvalues Ω of the different manifolds form bands. The separation between two consecutive bands is on the order of a molecular transition energy E, whereas the width of the n-exciton band is on the order of $4n$ times the typical intermolecular interaction V. Optical transitions are allowed only between consecutive bands. In the following, we only consider one-exciton states.

The one-exciton manifold of the aggregate of N molecules (two-level systems in this representation) consists of N states

$$|\sigma\rangle = \sum_i \varphi_{\sigma i}|i\rangle \tag{6}$$

where $\varphi_{\sigma i}$ is the ith component of the σth eigenvector of the matrix $\mathbf{H}_{ij}$. The corresponding eigenvalue Ω_σ gives the transition

frequency from ground state to $|\sigma\rangle$. To find the absorption spectrum, we use the transition dipole operator

$$\hat{P} = \sum_i \boldsymbol{\mu}_i(|i\rangle\langle 0| + |0\rangle\langle i|) \tag{7}$$

where μ_i is the transition dipole of the ith molecule. The transition dipole from the ground state to the one-exciton state $|\sigma\rangle$ is given by

$$\boldsymbol{\mu}_{0\sigma} = \langle 0|\hat{P}|\sigma\rangle = \sum_i \boldsymbol{\mu}_i \varphi_{\sigma i} \tag{8}$$

The intensity of the absorption at Ω_σ is proportional to the square of the transition dipole $\mu_{0\sigma}$. The resulting stick spectrum is usually dressed with a Lorentzian or Gaussian in order to get a smooth band. Analogously for the rotational strength at Ω_σ we have

$$r_{0\sigma} = \frac{\pi}{2\lambda_\sigma} \sum_{i,j} \boldsymbol{R}_{ij} \cdot (\boldsymbol{\mu}_i \times \boldsymbol{\mu}_j) \varphi_{\sigma i} \varphi_{\sigma j} \tag{9}$$

where λ_σ is the wavelength of the transition to state σ and $\mathbf{R}_{ij}$ is a vector from the ith molecule to the jth molecule. Due to $\mathbf{R}_{ij}$, a major contribution to r may originate from molecules which are far apart. At the same time, due to the disorder, $\langle i|\sigma\rangle\langle j|\sigma\rangle$ is falling off rapidly as a function of separation $\mathbf{R}_{ij}$ (vide infra). Even so, $\langle i|\sigma\rangle\langle j|\sigma\rangle$ usually has long low amplitude wings. These wings may therefore provide a major contribution to the circular dichroism spectra.

Due to the static disorder, the exciton states (6) are not perfectly delocalized over the full aggregate. The random distribution of Δ_i values causes a localization of the wave function to a limited region of the aggregate. There are a number of ways to characterize the extent of delocalization in molecular aggregates.[76] Often the inverse of the participation number[77] is used

$$\boldsymbol{L}(\sigma) = \sum_i \varphi_{\sigma i}^4 \tag{10}$$

For a localized state $L = 1$ and for a totally delocalized state L is of the order of $1/N$.

Alternatively the width of the spatial autocorrelation function $C_\sigma(n)$ of the wave function $|\sigma\rangle$ has been proposed as the measure of the extent of exciton delocalization in antenna systems:[70,78]

$$C_\sigma(n) = \langle \sum_i \varphi_{\sigma i} \varphi_{\sigma i+n} \rangle \tag{11}$$

where $\langle ... \rangle$ denotes an average over the different realizations of uncorrelated fluctuations Δ_i.

It has been pointed out that the antidiagonal cross section of the density matrix is the natural way to express the size of the exciton.[76] In a similar way Kühn and Sundström[79] defined the time-dependent exciton coherence length in terms of the density matrix in the site representation via a width of the function C_n

$$C_n(t) = \sum_i |\langle \rho_{i,i+n}(t) \rangle| \tag{12}$$

Besides the electronic Hamiltonian (5) with static disorder, there are also terms describing the electron−phonon interaction (dynamic disorder).[62] These are the terms which actually cause relaxation between exciton states. The electron−phonon interaction may be nonlocal, modulating the coupling term V, or it can be local, modulating the molecular energy E. The latter can be seen as a time dependence of Δ_i. These two qualitatively different electron−phonon coupling Hamiltonians read as

$$H^1_{\text{ex-ph}} = \sum_{ijq} F^q_{ij} \hbar \omega_q X_q |i\rangle\langle j| \tag{13}$$

$$H^2_{\text{ex-ph}} = \sum_{iq} \chi^q_i \hbar \omega_q X_q |i\rangle\langle i|$$

Here the phonons consist of both lattice modes and intramolecular (local) vibrations. χ_i^q and F_{ij}^q are the local and nonlocal linear electron−phonon coupling factors; ω_q and X_q are the frequency and the normal coordinate of the nuclear mode q. It turns out that these two types of electron phonon interaction have qualitatively different effects on the exciton relaxation. The local electron−phonon coupling only induces transitions if the phonon frequency is resonant with the exciton level separation, whereas in a modulation of the coupling term also the higher harmonic frequencies of a vibrational mode can lead to a resonance.[80]

Density Matrix Picture. Density matrix theory provides an universal treatment of the different regimes of dynamics.[65,79,81] In the approach called Redfield relaxation theory,[82,83] the dynamics of a few relevant degrees of freedom are handled explicitly (system), while the remaining degrees of freedom comprise a thermal bath (reservoir), which is weakly coupled to the system. A second-order perturbative treatment of the system-bath coupling together with tracing over the reservoir degrees of freedom yields the following equation for the reduced density matrix

$$\dot{\rho}_{ij}(t) = -i\omega_{ij}\rho_{ij} - \sum_{kl} R_{ij,kl}\rho_{kl}(t) \tag{14}$$

The first term on the right-hand side describes the coherent dynamics of the system due to its own Hamiltonian. The second term corresponds to the dissipative effects due to the interaction with the bath. Elements of the Redfield tensor $\mathbf{R}_{ij,kl}$ connect all density matrix elements. We can identify various different dissipative terms. $\mathbf{R}_{ii,jj}$ is the rate constant of the population transfer from jth state to the ith state (T_1 process in a Bloch model); $\mathbf{R}_{ij,ij}$ is the dephasing of the coherence between the ith states and jth states (T_2 process); $\mathbf{R}_{ij,kl}$ are general coherence transfer terms which do not have analogies in the optical Bloch equations. These coherence transfer terms were found to be important in understanding the survival of coherent nuclear motions in product states of curve crossing reactions[84] and also in light-harvesting systems.[85] The expressions for the Redfield tensor elements involve Fourier transforms of correlation functions of the system−bath interaction matrix elements. In the delocalized exciton basis, the electron phonon coupling terms of eq 13 lead to the following equations for the population transfer (exciton relaxation):[79,86]

$$R_{\beta\beta,\alpha\alpha} = -2\sum_{i\neq j} J_{ij}(\omega_{\alpha\beta})[|\varphi_{\alpha\, j}|^2|\varphi_{\beta\, i}|^2 + \varphi^*_{\alpha\, j}\,\varphi_{\beta\, i}\varphi^*_{\alpha\, i}\,\varphi_{\beta\, j}] \tag{15}$$

$$R_{\beta\beta,\alpha\alpha} = -2\sum_i J_{ii}(\omega_{\alpha\beta})|\varphi_{\alpha\, i}|^2|\varphi_{\beta\, i}|^2 \tag{16}$$

where

$$J_{ij}(\omega) = (1 + N(\omega))(f_{ij}(\omega) - f_{ij}(-\omega)) \tag{17}$$

$N(\omega)$ is the Bose−Einstein distribution function (thermal occupation number), and the spectral density f_{ij} is related to the

electron phonon coupling parameters F_{ij}^{q} and χ_i^{q} in (13). Equations 15 and 16 contain simple intuitive physics. In (16), the local fluctuations of an *i*th molecule cause the relaxation from exciton level α to β with a rate which is proportional to the extent of the involvement of the *i*th molecule in both exciton states and to the spectral density resonant with the exciton level spacing. Equation 15 suggests that the exciton relaxation slows down at the edges of the exciton band, since those states have the most localized character and if a molecule is involved in a nearly localized state then it is likely to have very little amplitude in another state. In the same way, this term should be efficient in the middle of the band, where delocalization is extensive. Analogously, we can conclude that the nonlocal fluctuations are very likely to induce transitions between two states which are well localized at two neighboring molecules. Because of (17) the back- and forward rates satisfy the detailed balance relation.

Similarly, for the localized molecular basis we would obtain the rate terms $R_{ii,jj}$ which describe the hopping of excitation from the *j*th molecule to the *i*th molecule. However, in the Redfield theory, we would not recover the Förster (1) exactly, since the system−bath interaction is only treated to second order, meaning that the multiphonon transitions are neglected. At the same time, in the spectral overlap integral Θ of (1) in principle all orders of the electron−phonon interaction are present and multiphonon transitions, if they exist, are included.

Diagonal Disorder and the Dipole Strength of the Lowest Exciton State of LH2. In the perfect exciton model the excitonic states of the LH2 ring are calculated by diagonalization of the Hamiltonian (5), where all the site energies have been chosen to be identical. In such a model, the lowest excitonic state gains very little dipole strength, since all the dipoles are almost in the plane of the ring. By far the largest part of the dipole strength is collected in the next degenerate pair of excitonic states, the $k = \pm 1$ states, and all the other states contain no (or very little) dipole strength. In such a scheme, the low-temperature radiative rate from the lowest level would be negligible and the state would not be fluorescent. Experiments with LH2 from *Rb. sphaeroides* and *Rps. capsulatus* have shown that this is not the case;[70] in fact, at 4K, the dipole strength of the emitting state of LH2 corresponds to about 2−3 monomeric BChls. Moreover, the dipole strength of the emitting state is more or less independent of temperature (see Figure 3). To explain this discrepancy it was assumed that in LH2 the site energies of the BChls are distributed in a Gaussian fashion, due to some small fluctuations in the pigment protein structure that modulate the transition frequency. If these fluctuations are "static", i.e., they vary on a time scale much slower than the fluorescence (which of course is not really true, see below), then one can calculate the linear optical properties of the LH2 ring by averaging the outcome of the diagonalization procedure over all possible realizations of the energetic disorder. The temperature effect is modeled by assuming that the excited-state relaxation creates a Boltzmann distribution over the various exciton states. The result of such a calculation is also shown in Figure 3 for various values of the ratio of the disorder σ vs the dipole−dipole coupling strength V. For $\sigma/V = 0$, one obtains at $T = 0$ the "forbidden" dipole of the lowest excitonic state. As T increases, the strongly allowed $k = \pm 1$ states become more and more populated thereby increasing the radiative rate of the complex; at about 60 K a maximum radiative rate is reached. For higher temperatures, the excitonic effect is gradually lost: for $T \rightarrow \infty$ the radiative strength would be 1 and the excitation would be fully localized on monomers. For increasing values of σ/V, already at $T = 0$ the various exciton states are mixed, thereby adding dipole strength to the lowest state of LH2. Furthermore, the effect of increasing T is reduced. For $\sigma/V = 2$ and at 0 K, the emitting dipole strength is about 2−3 times the monomeric value and this value hardly changes with temperature between 0 and 300 K, in agreement with experiment. The calculation demonstrates that disorder in the site energies is an essential ingredient to understand the spectroscopy of LH2, and its major effect is that it destroys the "delocalized exciton" picture that was advanced by some authors.[45,87,92]

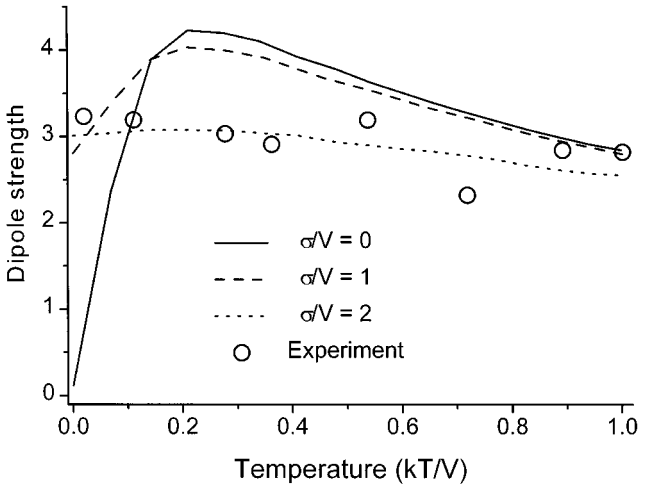

Figure 3. Experimental (squares) and calculated (lines) temperature dependence of the emitting dipole strength of LH2 ring relative to the dipole strength of a BChl *a* monomer. Three different values of σ/V were used in calculations: 0 (solid), 1 (dotted), 2 (dashed). σ is the fwhm of Gaussian distribution of site energies. (Taken from ref 79.)

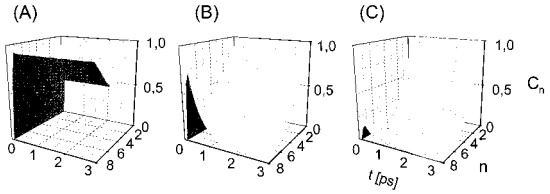

Figure 4. The one-exciton coherences created by Fourier transform limited 90 fs laser pulse at 850 nm in LH2 ring according to eq 12. (A) a homogeneous system without electron−phonon interaction. (B) Homogeneous system with electron−phonon coupling 50 cm^{-1}, the spectral density has a maximum at 100 cm^{-1}, $T = 280$ K. (C) Electron phonon coupling as in B and spectral inhomogeneity with fwhm ~700 cm^{-1}. (Taken from ref 79.)

Localization of the Exciton in the Presence of Static and Dynamic Disorder. We saw how the static disorder destroys the perfect delocalization of the exciton states. It is clear that electron−phonon interaction (13) (dynamic disorder) in general further localizes the states. To study the effect of weak electron−phonon coupling on the initially created coherent superposition of exciton states, the localization of the function $C_n(t)$ of eq 12 for B850 molecules of LH2 was calculated for various parameter sets (see the caption of Figure 4).[79] Part A of Figure 4 corresponds to the ideal case without disorder. The symmetry of the exciton states of a ring gives $C_n(t)$ a sinusoidal form reflecting a fully coherent excitation, which does not change with time after the pump pulse is over. If we switch on the electron−phonon coupling (part B in Figure 4), we see that the initial coherence over the ring is not fully established since the dephasing and relaxation are effective already during the pulse. We observe how the system rapidly relaxes toward an equilibrium distribution which leads to an almost complete decay of $C_n(t)$ for larger n. We point out here that the equilibrium state

reached in Figure 4 does not imply that we have nonzero off-diagonal elements of the density matrix in the delocalized exciton basis. In fact we have an incoherent superposition of thermalized excitonic eigenstates (6). Finally, if we include both static and dynamic disorder we see that the long range coherence initially created by the laser pulse is further suppressed (part C of Figure 4). Comparison with the homogeneous case (middle part) reveals that the final function is narrower if disorder is taken into account. This suggests that disorder plays a stronger localizing role than the electron−phonon interaction in B850 and already the initially created exciton has a rather localized character. A similar conclusion was recently made in a theoretical work based on the comparison of the superradiance in J-aggregates and in light-harvesting systems.[88]

The behavior of $C_n(t)$ reflects the dynamic exciton delocalization. If we take the full width at half-maximum of $C_n(t)$ as the extent of exciton delocalization, we can estimate from the part C of Figure 4, which corresponds to the parameters of the B850 ring of LH2, that the excitation is coherent over about four monomeric BChl molecules. A similar number has been suggested based on various other methods: analyses of the absorption difference line shapes,[79,89] superradiance (see previous section),[70] theoretical considerations,[90] and the amount of induced absorption per absorbed photon.[91]

Calculation of the LH2 CD-Spectrum Using Exciton Theory. As a further application of exciton theory and examination of the consequences of disorder to spectral properties, we discuss the CD spectrum of LH2. All LH2 complexes exhibit strong CD signals in the region of their main absorption bands and traditionally these CD signals have been correlated with the presence of strong excitonic interactions. Given the high-resolution structure and assuming that the physical model that describes the spectroscopy of this system is correct, we should be able to calculate the CD spectrum of this complex. The LH2 CD exhibits a number of features. First, there is a strong, generally conservative spectrum in the 850 nm region (positive rotational strength on the blue side, negative on the red side) with a remarkable property, namely, that the zero crossing of the CD spectrum does not coincide with the absorption maximum but is at about 6−7 nm longer wavelength.[92,93] Second, there is a complicated spectrum in the 800 nm region, which not only varies from species to species, but also dramatically depends on the chemical conditions of the complex (e.g., the type of detergent used for the biochemical purification). Recently, Koolhaas et al.[94] identified a broad negative band around 780 nm in the CD spectrum of a B800-less mutant as originating from the upper exciton band edge of the B850 ring. A calculation of this CD spectrum, including the redshifted zero crossing, always required the full ring. The reason is simple: for the perfect ring-like aggregate (no disorder) with the transition dipoles more or less in the plane of the ring, the lowest optical transition becomes (almost) optically forbidden, while the absorption is concentrated in the next two degenerate exciton states. However, the rotational strength of the lowest level and the two allowed levels is similar, but with a sign change. As a consequence, the CD zero crossing is to the red of the absorption maximum. The inclusion of disorder in the calculation destroys the forbidden character of the lowest excitonic state (see below), but the position of the zero crossing carries the memory of the original "perfect" ring.[95] The experimental spectrum of the B800-less LH2 of *Rb. sphaeroides* could be very well modeled using the excitonic expressions for CD. A representative example of the calculated CD spectrum of this mutant is shown in Figure 5 together with the measured CD spectrum. The

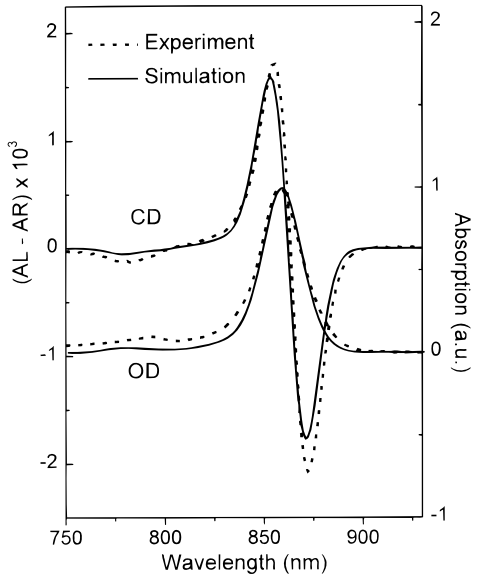

Figure 5. Experimental (dotted) and calculated (solid) absorption and CD spectra of the B800-less mutant of *Rb. sphaeroides* at 77 K. In the mutant the alpha polypeptide was shortened by two amino acids, thereby destabilizing the B800 binding site. In calculations, the following parameters were used: the fwhm of the inhomogeneous broadening and homogeneous broadening is 500 and 200 cm^{-1}, respectively; the inhomogeneous distribution of site energies has a mean at 813 nm; the mean nearest neighbor interaction energy is 300 cm^{-1}. The beta bound BChls are rotated away from the plane of the ring and the alpha bound BChls are rotated toward the plane of the ring by 7°. (Based on ref 94.)

assumed dielectric constant was 1.2, the fwhm for the inhomogeneous broadening was 500 cm^{-1} and for the homogeneous broadening 200 cm^{-1}. Note that the precise positioning of the upper edge of exciton band allowed an accurate estimate of the magnitude of the nearest neighbor dipole−dipole coupling matrix elements, which were found to be 300 and 230 cm^{-1} between α and β and β and α chromophores, respectively. We finally note that an even better fit to the experimental CD spectrum could be obtained by allowing one of the transition dipoles to be tilted slightly toward (α-B850) or away (β-B850) from the plane of the ring.

4. Interactions and Energy Transfer between Carotenoid and Bacteriochlorophyll Molecules of LH2

Carotenoid molecules in photosynthetic pigment−protein complexes in general have two major functions: photoprotection[96] against triplet states and singlet oxygen, and light harvesting.[15,97,98,99,100,101] Frequently, as is also suggested by the LH2 crystal structure, carotenoids have a structural function of stabilizing the pigment−protein of which they are a part. Here we will limit our discussion to the light-harvesting function, with the aim of revealing the mechanisms of energy transfer and pathways of energy flow between the carotenoid and BChl molecules of the LH2 complex. Due to their conjugated π-electron systems and electronic structure, carotenoid molecules are known to be very sensitive to electric fields.[102−104] Electrochromic band shift measurements of carotenoid absorption spectra have therefore been extensively used to report on electron transfer processes and membrane organization. It was recently discovered that carotenoids also sense changes of local electric fields associated with optical excitation of nearby pigment molecules (BChls).[105] We will briefly discuss how this property of carotenoids may be used to monitor excitation transfer dynamics in a LH complex. Several recent review

articles have appeared on carotenoid light-harvesting,[15,97−101] and we refer to them for an account of earlier work. Here we will discuss the most recent progress and status of the topic.

From the crystal structure of LH2 (Figures 1 and 2), it is immediately apparent that carotenoid molecules, being very well integrated into the protein and coming within very short distance of both the B800 and B850 BChl molecules, are ideally located for performing their two major functions. The closest distance from a carotenoid molecule (the fully resolved Crt in the structure) to the central Mg atom of a BChl molecule is 9.3 Å for B800, 5.44 Å for the Mg atom of the α-B850, and 8.04 Å for the β-B850 Mg atom.[106] Similar short distances were hypothesized for the partially resolved Crt molecule in LH2.[106] Several shorter, nonbonded contacts between Crt atoms and atoms of the BChl macrocycles (∼3.5−5 Å), of potential importance for exchange interactions, are also observed in the structure.

An inspection of the crystal structure for Crt−BChl chromophore distances and orientations is quite informative as a starting point for a discussion on the mechanisms and channels of excitation transfer in LH2. Here we will limit our focus to the fully resolved Crt molecule in the LH2 structure. In considering dipole−dipole interactions, the relative orientations of the transition dipole moments are important. From Figure 2 it is seen that the Crt backbone (and thus the $S_0 \rightarrow S_2$ transition dipole) is essentially parallel with the B850 BChl $S_0 \rightarrow Q_x$ transition moment and perpendicular with all the other BChl (both B800 and B850) Q_y and Q_x transition dipoles. This suggests that Crt $S_2 \rightarrow$ B850 Q_x energy transfer could be quite efficient and proceed via the Förster mechanism, while all the other transfer channels from Crt S_2 should be considerably less efficient. The Crt S_2 state is known to decay very quickly (∼200 fs)[107] via internal conversion to the optically forbidden S_1 ($2A_g$-) state. So even with an efficient Crt $S_2 \rightarrow$ BChl Q_x transfer channel it is likely that some fraction of the energy would end up in the lowest excited Crt S_1 state. The dipole forbidden nature of this transition has triggered the suggestion that energy transfer from this state to the BChls does not occur via the Förster mechanism, but rather via electron exchange.[15] However, as we will see below, more recent calculations suggest that even at these relative short distances, the Dexter exchange mechanism is very inefficient and that higher order Coulombic (quadrupole−dipole) and polarization interactions may perhaps account for a transfer channel from Crt S_1 to BChl, still with a reasonable rate (time constants on the time scale of tens of picoseconds).[108,109] Already at the outset of this discussion we would like to note that although several recent time-resolved spectroscopic measurements have shed new light on photosynthetic light-harvesting involving carotenoids, there remains a considerable number of issues lacking a consensus understanding.

The overall efficiency of Crt to BChl energy transfer is highly variable, ranging from close to 100% in LH2 of *Rb. sphaeroides* and *Rps. acidophila*[110−112] (and several similar complexes) to as low as ∼30% in LH1 of *Rs. rubrum*.[111] The very low efficiencies appear (at least partially) to be the result of a remarkable fission process of the Crt singlet states followed by formation of triplets and ensuing quenching processes.[113] We will not consider this latter case here, but focus on the actual light-harvesting processes.

From the structure of LH2 it appears that excitation energy could be transferred from the Crt to both the B800 and B850 BChl molecules. Already quite early steady-state measurements of excitation spectra of the intact LH2 complex of *Rb. sphaeroides* and on the complex lacking B800[13,114] showed that approximately 75% of the energy absorbed by the carotenoids is transferred directly to B850, while the remaining 25% passes via B800 before it ends up on B850 through the B800 → B850 channel discussed below (section 6). Similar values for the relative distribution of energy going through the two B850/B800 channels has been observed for LH2 of *Rps. acidophila.*[115] Time-resolved results available so far have not provided more direct information on this issue, but they are not inconsistent with the steady-state results.

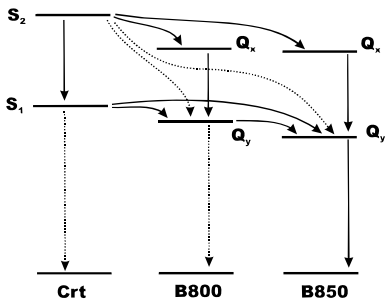

Figure 6. Scheme of the energy levels together with excitation transfer and relaxation processes involved in LH2. Solid lines show the major and dotted lines the minor transfer/relaxation channels. We point out that the precise position of Crt S_1 energy level is not known.

The extremely low fluorescence yield (and consequently very fast deactivation) of the Crt S_2 (B_u^+) state suggested initially that most of the energy transfer from the Crt to the BChl occurs from the Crt S_1 ($2A_g^-$) optically forbidden state (Figure 6). As was mentioned above, this was taken to indicate that the Dexter electron exchange mechanism is operative for this process.[15] This belief appeared to be confirmed by the first time-resolved measurements of the Crt → BChl energy transfer process, where the Crt absorption at 480 nm in LH2 of *Rps. acidophila* was seen to recover with a 5.6 ± 0.9 ps time constant following excitation with a 4 ps pulse at 515 nm.[116] Later transient absorption measurements on LH2 of *Rb. sphaeroides* by Trautman et al.[117] and by Shreve et al.,[22] with better time resolution (200−300 fs pulses), showed that following Crt excitation the B850 Q_y state was populated within 200 fs. Similar time-resolved measurements by the same group on β-carotene showed that Crt $S_2 \rightarrow S_1$ internal conversion occurs on the same time scale (∼200 fs).[107] These two results suggested that in LH2 the Crt S_2 state may be deactivated by two competing channels, Crt $S_2 \rightarrow$ B850 and Crt $S_2 \rightarrow$ Crt $S_1 \rightarrow$ B850/B800 Q_y (see Figure 6). The relative contributions of the two channels would be determined by the ratio of the rates of the processes Crt $S_2 \rightarrow$ B850 and Crt $S_2 \rightarrow$ Crt S_1. Shreve et al.[22] also addressed the problem of Crt → B800 transfer in LH2, and showed that, by exciting the Crt absorption band of *Rb. sphaeroides* LH2 with a ∼200 fs 510 nm pulse and detecting the transient absorption changes in the B800 absorption band, energy was efficiently transferred to B800 from the Crt. To interpret the observed kinetics a model was suggested involving energy transfer to B800, both directly from the Crt S_2 ($\tau = 1.7$ ps) and indirectly via the Crt S_1 state ($\tau = 3.8$ ps). Using a 9.1 ps lifetime of the Crt $2A_g^-$ state (as measured for spheroidene in cyclohexane solution) this model predicts an overall efficiency of 75% for the energy transfer Crt $S_2 \rightarrow$ B800 → B850. When taking into account that $^3/_4$ of the carotenoids transfer their energy to B850 with probably close to unit efficiency (as suggested by steady-state mesurements[13]), these results are in good agreement with the observed overall Crt to B850 transfer efficiency of ∼95%.

In a set of transient absorption measurements on LH2 and whole chromatophores of *Chr. purpuratum*, Andersson et al.[118] also addressed the question of pathways of energy transfer from

Crt to BChl. Following excitation of the Crt (okenone in this species) at 580−590 nm with a ∼200 fs pulse, kinetics and transient absorption spectra were measured over the wavelength range 400−900 nm, and characteristic features of both B800 and B830 (the B850 of *Chr. purpuratum*) excited-state populations were observed, suggesting direct energy transfer from Crt to both B800 and B830. On the basis of their results, a model was constructed in which one Crt molecule is coupled to B830 and transfers energy with a time constant of 50−100 fs directly from Crt S_2 to B830 Q_x. According to the model, a minor amount of the energy absorbed by this Crt is transferred to the B830 Q_y state via the Crt S_1 state with a time constant of 3.8 ps. Another Crt molecule is assumed to be coupled to the B800 BChl molecule, and transfer occurs exclusively via the Crt S_1 state to B800 Q_y. These channels of Crt to B830/B800 energy transfer would basically obey the "most favored" processes as suggested by the alignment of Crt and BChl transition dipole moments, as mentioned at the beginning of this section. No information about the ratio between the B800/B830 channels could be obtained from these measurements, but the results were also consistent with the 25/75 B800/B850 ratio suggested by steady-state measurements.[13,114] For definite assignment of energy transfer processes a correlation of donor decay and acceptor rise times is necessary. Due to limited time resolution and nonlinear excitation-excitation annihilation (giving rise to additional kinetic components on the picosecond time scale) this could not be done in these measurements. Until this has been performed the assignments must be considered as tentative.

In a pigment system, such as LH2, containing several distinct chromophores, transient absorption measurements often result in quite complex mixture of different signals, which may be difficult to interpret. Time-resolved fluorescence may provide a somewhat simpler picture. Using the femtosecond fluorescence upconversion technique, Fleming and co-workers addressed the question of direct Crt $S_2 \rightarrow$ BChl energy transfer. In a first investigation[119] on LH2 and LH1 of *Rb. sphaeroides* the Crt S_2 fluorescence was observed to decay with a major (95% amplitude) time constant of 80 fs for LH2 and 55 fs for LH1. A minor 225−300 fs (5% amplitude) decay component was assigned to inactive Crt molecules. Upon combining these results with a measurement of the Crt S_2 fluorescence decay in various organic solvents (τ = 150−225 fs, which measures the Crt $S_2 \rightarrow$ Crt S_1 decay), it was tentatively concluded that direct energy transfer from Crt S_2 to BChl Q_x occurs with a time constant of 170 fs for LH2 and 90 fs for LH1, which would result in a substantial fraction of the energy absorbed by the Crt molecules to go along the direct channel from Crt S_2 to BChl Q_x (see Figure 6). However, it was also pointed out that the value used for the Crt $S_2 \rightarrow S_1$ internal conversion process is that obtained with the Crt (spheroidene) in solution, and if the rate of this process would be modified by the protein the energy transfer process could have substantially different rates.

In more recent work from the Fleming group,[120] this time on the B800−B820 LH2 complex of *Rps. acidophila*, the Crt → BChl energy transfer pathways and efficiencies were studied in more detail and the measured energy transfer rates were compared with calculations in order to obtain mechanistic information. Again, femtosecond fluorescence upconversion measurements were used to monitor the decay of the Crt (rhodopin glucoside) S_2 fluorescence and the corresponding rise and decay of the B820 fluorescence. The Crt S_2 fluorescence detected at 550 nm was observed to decay with a 54 ± 8 fs (amplitude 98%) time constant and the temporal evolution of the B820 fluorescence could be described by a 90−150 fs rise time (wavelength dependent in the range 830−850 nm) and two decay times 1−4 ps and 16 − >100 ps (also wavelength dependent with the longer time constants observed at the redder wavelengths). These results were taken as evidence for fast 65−130 fs Crt $S_2 \rightarrow$ B820 Q_x energy transfer, using a value of 120−150 fs for the Crt $S_2 \rightarrow S_1$ internal conversion. From fits of the B820 fluorescence kinetics an attempt was made to obtain some information about the rate and contribution of the Crt $S_2 \rightarrow S_1 \rightarrow$ B820 Q_y channel. However, the complications added to the kinetics by an unknown amount of excitation−excitation annihilation in B820 (giving rise to picosecond decay components in addition to those associated with the energy transfer), made this impossible. Using a value of 75% for the overall Crt to BChl energy transfer efficiency[121] it could nevertheless be concluded that Crt S_1 to BChl Q_y energy transfer occurs with a time constant of 3−15 ps in this complex, leading to the efficiencies 48−70% of the Crt $S_2 \rightarrow$ B820 Q_x energy transfer and 27−5% of the Crt $S_1 \rightarrow$ B800/B820 Q_y channel, and 25% of the energy lost. The measured rates of Crt to BChl energy transfer were compared with calculations of couplings and spectral overlaps. For the couplings involving the strongly optically allowed transitions both the conventional point dipole description as well as a more realistic, so-called transition density cube method were used.[73] In the latter method, the vector description of the transition dipole moments of the interacting molecules is replaced by three-dimensional transition density volumes, and interactions between these volumes are calculated. This approach is expected to give a more accurate description of the interaction between molecules at short distances and for the Crt molecules where the transition dipole vector may not coincide with the molecular framework. For calculations of the Crt S_1 − BChl Q_y interactions, methods developed by Scholes et al.[109] were used. The calculations suggested short Crt $S_2 \rightarrow$ BChl Q_x transfer times of similar magnitude (∼240 fs) as those observed experimentally and much slower Crt $S_1 \rightarrow$ BChl Q_y transfer (∼32 ps). The latter, nevertheless, of the same order of magnitude as indicated by the experiments. The calculations of the Crt S_1 − BChl Q_y interactions suggested that this coupling is accounted for by a combination of Coulombic (quadrupole−dipole) and polarization interactions and that electron exchange interactions are much weaker. The latter result agrees with calculations of Nagae et al.[108]

We conclude this section on carotenoids by briefly discussing some recent results of ultrafast carotenoid band shifts. Following excitation with a femtosecond pulse of the BChl Q_y bands of B800 and B850 of LH2 of *Rb. sphaeroides*, distinct changes in the carotenoid S_2 absorption spectrum between 430 and 530 nm were observed.[105] Femtosecond transient absorption spectra and kinetics were measured, revealing an ultrafast carotenoid response to the excited BChl pigments. The observed Crt response was interpreted as a Crt electrochromic response to the induced local electric fields from the photoexcited BChl B800 and B850 molecules. The change in dipole moment ($\Delta\mu_{B800}$ ∼1 D; $\Delta\mu_{B850}$ ∼3 D[122]) upon excitation creates an electric field change of the order of 10^8 V/cm at a distance of ∼5 Å from the BChl molecule, according to a simple point dipole approximation. Since the field strength falls off with a r^{-3} distance dependence, even at 20 Å from the excited BChl molecule the field strength is similar to the uniform transmembrane fields used in Stark and ion gradient experiments of Crt electrochromic band shifts.[123−125] The response of the Crt to the local field is different when the excitation is located on B800 and B850, respectively. The B800 to B850 energy transfer was reflected as a decay of the amplitude of the Crt response,

with a time constant exactly matching the B800 → B850 energy transfer. The temporal evolution of the Crt-shift spectrum also clearly demonstrated the different response of the two carotenoid molecules in LH2. These results are indicative of a new property of carotenoids that is manifested as a unique ability to detect and report changes in their immediate environment, thereby serving as sensitive probes of local dynamics and structure.

5. Energy Transfer among the B800 Bacteriochlorophylls in LH2

Upon studying the structures of LH2 of *Rps. acidophila* and *Rs. molischianum*, it is clear that the interaction between B800 pigments is sufficiently weak to avoid excitonic effects, while at the same time sufficiently strong to allow fast energy transfer, assuming a reasonable value for the overlap between B800 emission and B800 absorption.[13,33,36,126] Experimentally, several groups have reported the presence of an additional relaxation processes in the B800 band of LH2 besides the main B800 to B850 transfer. In general the evidence was most clear at low temperatures and intraband excitation transfer and/or vibrational relaxation were suggested as possible kinetic processes. The earliest observation originates from the work of Kramer et al.,[13] who reported that, upon Q_x excitation of LH2 at 4 K, the resulting fluorescence from B800 was largely depolarized. Given that there is a ∼1.5−2 ps energy transfer from B800 to B850 at 4 K, this observation implied that within the ∼1.5 ps lifetime at least a few energy transfer events between differently oriented B800s had to take place to cause the depolarization, and as a consequence the rate of B800→B800 energy transfer was crudely estimated to be about 500 fs. It is worth mentioning that in the original 1984 Kramer model this translated into a B800−B800 distance of about 21 Å, very similar to the 1995 crystallographic value.[45]

Direct evidence for B800−B800 transfer in *Rb. sphaeroides* and *Rps. palustris* was first obtained at room temperature by Hess et al.[23] who observed in femtosecond pump−probe measurements a clear anisotropy decay with a time constant of about 1 ps. This time constant appeared to be too slow to explain the fluorescence depolarization by Kramer et al.[13] At the end of the chapter we provide a possible explanation to this discrepancy. The authors also observed a fast ∼300 fs component in the isotropic decay of B800, which was assigned to energy transfer between almost parallel B800 molecules and possibly to vibrational relaxation.

Time-resolved experiments on a variety of LH2 systems largely confirmed the presence of a fast relaxation process in the B800 band at low temperatures.[32,34,36,126] In LH2 of *Rb. sphaeroides*, Hess et al. found a 300 fs relaxation channel in both isotropic and anisotropic decays. The results were modeled as a hopping in a ring with an average pairwise nearest neighbor transfer time of 350 fs.[126] In the same LH2, Monshouwer et al. found that in the blue wing of the B800 absorption profile the major isotropic decay occurred with a 400−500 fs lifetime component, which perfectly matched a rise time in the red tail (see Figure 7).[24,36] A very similar 400 fs intraband relaxation process was observed by Wu et al.[32] for B800 in LH2 of *Rps. acidophila* at 19 K and recently for the B800−820 LH2 from *Rps. acidophila* by Ma et al.[35] The latter authors also observed a very similar phase in the low-temperature anisotropy decay, measured at the same probing wavelength. Also, recent work by Wendling et al.[37] at 77 K on B800−850 LH2 of *Rps. acidophila* is fully consistent with a ∼500 fs blue to red relaxation and an anisotropy decay with a closely related time constant. In the B800 band of LH2 of *Rs. molischianum*[37] studied at 77 K, both the blue-to-red isotropic decay and the absorption anisotropy decay occur in about 0.8−0.9 ps, a factor of 2 slower than observed in LH2 of *Rps. acidophila* and *Rb. sphaeroides*.

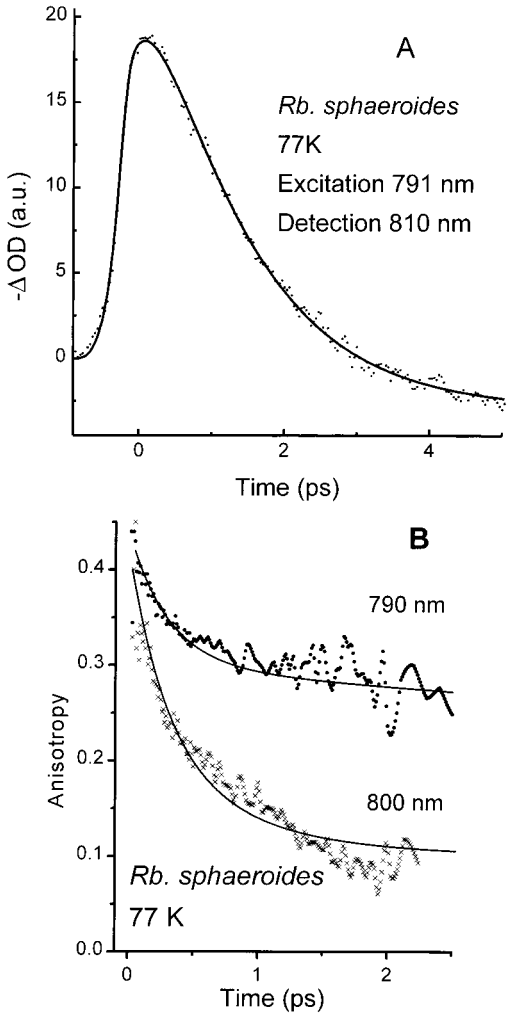

Figure 7. (A) Two-color pump−probe measurement in the B800 band of *Rb. sphaeroides* at 77 K. Excitation is at blue and detection at red side of the band. The solid line is a fit with a rise of 440 fs, reflecting downhill energy transfer among B800's, and a 1.3 ps decay, due to B800 → B850 transfer. (Taken from ref 36.) (B) Anisotropy decay of B800 of *Rb. sphaeroides* at 77 K. The solid curves represent the fit with a two-exponential decay with time constants 0.3 and 1.5 ps with amplitudes 0.12/0.2 and 0.08/0.1, respectively, and a constant level 0.2/0.1 at 790/800 nm. (Taken from ref 126.)

The existence of a fast relaxation process in the B800 band at low temperature is supported also by hole-burning experiments.[28,127] It was found that upon burning a hole in the red tail of the B800 absorption band, a lifetime limited value of 2−2.5 ps for the holewidth was obtained. The 2−2.5 ps process was ascribed to energy transfer from the low-energy B800s to B850. Scanning the burning wavelength to the blue, for $\lambda <$ 798 nm gradually broader holes were obtained, eventually corresponding to a lifetime of 0.9 ps at $\lambda_b = 790$ nm. A deconvolution of the holewidth vs burning wavelength spectrum demonstrated that about one-third of the B800 pigments were responsible for the 2.0−2.5 ps lifetime; the remaining B800s were relaxing faster. On the basis of the B800-emission depolarization results, the faster decays in the blue part of the B800 absorption band were interpreted as blue-to-red energy transfer within the B800 band. In fact very similar results were

obtained by Wu et al.,[32] but they favored an explanation, partly based on the observed pressure effect, in which the faster relaxation of the blue B800s was a manifestation of their coupling to the high exciton manifold of the B850 ring. We would also like to comment on the fact that the hole burning appears to yield longer time constants than the time-resolved methods (see also section 6 on B800 to B850 transfer). The hole-burning yield is proportional to the lifetime of the excited state. In our systems, we are likely to have broad distributions of the transfer rates instead of a single rate. This may imply that in hole burning we preferably pick the molecules with longer lifetimes and therefore observe systematically slower transfer phases than the average transfer time.

As mentioned above, at room temperature the rate of energy transfer among the B800's appears to slow.[23] However, due to the fact that the time window available for the observation of the depolarization has significantly shortened at room temperature as a result of the faster B800 → B850 energy transfer (see below), the results here are not as consistent as for low temperature. Ma et al.[34] report 300-400 fs anisotropy decays in the B800 band of LH2 (B800−850) of *Rps. acidophila* at room temperature, but the same group reports an anisotropy decay of more than 1 ps in the closely related B800−820 of the same purple bacterium.[35] This latter value is close to the value by Hess et al. for LH2 of *Rb. sphaeroides*[23] and Kennis at al. for LH2 (B800−850) of *Rps. acidophila.*[128] Photon echo and transient grating experiments on LH2 of *Rb. sphaeroides* by Joo et al.[129] have also been taken to reflect rather slow energy transfer among the B800's at room temperature.

In general, we believe that energy transfer within the B800 ring can be well understood on the basis of the Förster equation for energy transfer in the weak coupling limit. For LH2 of *Rps. acidophila*, the estimated nearest neighbor coupling is about 25 cm^{-1}, which is 1 order of magnitude less than the site inhomogeneity (about 150 cm^{-1}) and the electron−phonon coupling. Quantitative estimates of the rate of B800−B800 energy transfer systematically arrive at numbers in the range of a few hundred femtoseconds[27,73] up to 1 ps.[32,36] Since for the isotropic low-temperature experiments the observed decay reflects the sum of all possible decay paths, i.e. for a blue B800 energy transfer to two neighbors plus downhill energy transfer to B850, a neighbor-to-neighbor transfer rate of 0.5−1 ps would be more than sufficient to account for the experimental observations. Similarly, the anisotropy decay measurements at 77 K by Hess et al.[126] yielded an average nearest neighbor pairwise transfer time of 300−400 fs. The Förster equation correctly predicts the difference in the B800→B800 energy transfer rate between *Rps. acidophila* and *Rs. molischianum*, the latter being about 2-fold slower due to the smaller dipole−dipole coupling (see Table 1; note that the rate scales with the square of the coupling matrix element). And perhaps most importantly, the temperature dependence of the Förster overlap integral can explain the decrease of the B800 to B800 transfer rate at room temperature. Calculations predict that due to the broadening of the homogeneous bands the transfer rate decreases between 77 K and room temperature.[27,126]

6. B800 to B850 Energy Transfer

This transfer step is probably one of the best studied kinetic processes in bacterial light harvesting. Early time-resolved experiments found that excitation transfer from B800 to B850 in *Rb. sphaeroides* occurs on a picosecond or shorter time scale.[18,130] In subsequent work with subpicosecond resolution, Shreve et al.[22] estimated the transfer step to be 0.7 ps at room

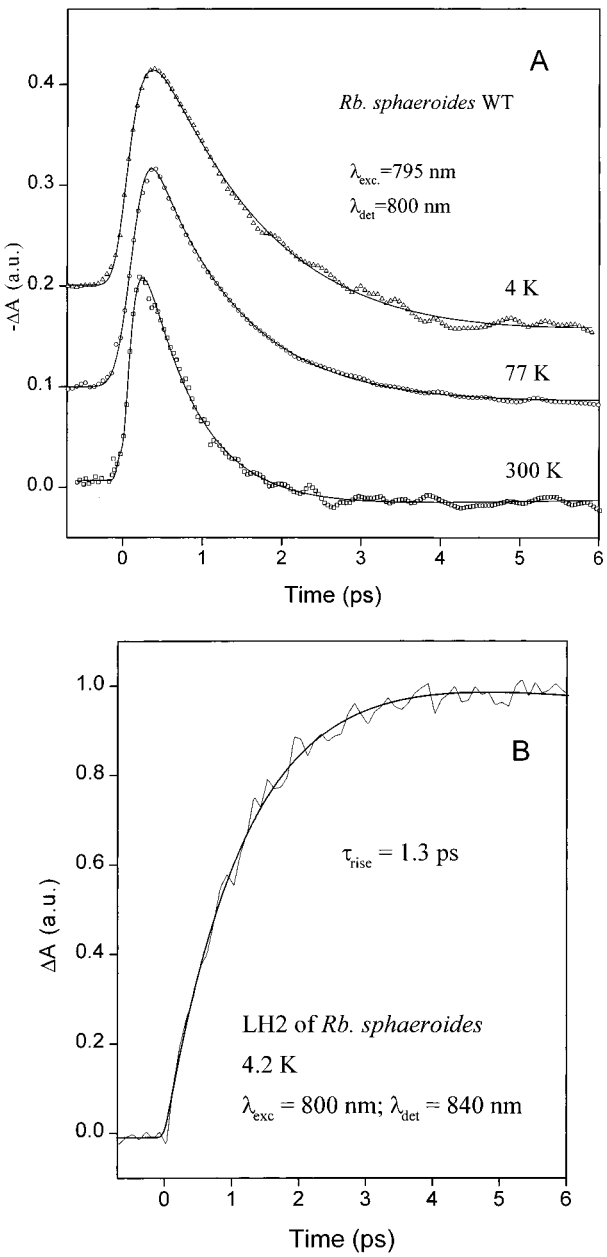

Figure 8. (A) Two-color transient absorption signals in chromatophores of *Rb. sphaeroides* at three different temperatures. Pump and probe wavelengths are 795 and 800 nm, respectively. The kinetics were fit with a sum of three exponentials. The shortest time ∼0.3 ps is the same in all curves and reflects the internal dynamics in B800. The second time constant was 0.7 ps at 300 K, 1.2 ps at 77 K and 1.5 ps at 4 K; it corresponds to B800 → B850 transfer. The third time constant is long and corresponds to the decay of the excitation in B850. (B) 4 K transient absorption signal with pump and probe wavelengths at 800 and 840 nm. The kinetics have a rising component with time constant 1.3 ps. (Taken from ref 27.)

temperature. This time constant has been confirmed a number of times with femtosecond time resolution.[23,27,129,131] A very similar rate for B800 to B850 transfer has also been found in two different LH2 complexes from *Rps. acidophila*.[34,35] For all species studied it was reported that the transfer time increases upon lowering the temperature, being 1.2 ps at 77 K[24,27] and 1.5 ps at 4 K[27] in *Rb. sphaeroides* (see Figure 8). Note that somewhat longer transfer times were extracted from hole burning measurements at 4 K.[25,26]

The B800−B850 coupling of ∼30 cm^{-1} suggests that the transfer occurs via the incoherent Förster transfer mechanism.

It was realized that the spectral overlap where only 0−0 transitions of a donor and acceptor are involved is not large enough to explain the fast B800 to B850 transfer because of a relatively large energy gap and it was suggested that certain BChl *a* vibrational modes are involved in this step.[26] To examine this process in some detail, the B800 → B850 transfer was measured in a series of mutants with gradually blue-shifted B850[25,132] and B800[133] absorption bands. A single or double mutation of the tyrosine+13−tyrosine+14 motif of the α-polypeptide of LH2 of *Rb. sphaeroides* results in a shift of B850 to B839 and B826,[7] respectively. In a similar way, mutation of βArg-10 blue shifts the B800 band.[133] The experimentally observed variations of B800 → B850 transfer times with the energy gap between the donor and acceptor pigments of LH2 measured at 77 K was qualitatively reproduced by spectral overlap calculations.[132−134] Also, the measured temperature dependence of the B800 → B850 transfer time could be accounted for with these calculations using the Förster transfer model. However, the above calculations did not provide an absolute value of the transfer rate. A more recent and quantitative Förster calculation of this energy transfer step[22,73] using reasonable values for the Franck−Condon factors of the vibrational modes of BChl *a*, which are essential to account for the spectral overlap between the B800 fluorescence and the B850 absorption, gave a B800 → B850 transfer time which is considerably longer than the measured one, suggesting that some additional channel may be operative in the B800 → B850 process. On the basis of hole-burning experiments at high pressure[32] and Redfield theory calculations[86] it was suggested that this additional channel could be the interaction of the B800 excited state with the upper exciton band edge of B850. Indeed, several studies have suggested that the weakly allowed higher edge of the B850 exciton band could be resonant with B800. For example, Wu et al.[32] found that the change of the cutoff between narrow and wide spectral holes burned into the B800 band correlated with the pressure shift of the B850 band relative to the B800 band, suggesting that an upper excitonic component of B850 is shifting under the B800 band. Pullerits et al.[27] analyzed the shape of the B800 absorption spectrum and concluded that it cannot be reproduced by the known spectral properties of BChl *a* suggesting that a considerable amount of the blue wing absorption of B800 originates from the B850 upper exciton component. Recent CD measurements on LH2 antenna complexes from a B800-less mutant of *Rb. sphaeroides* have provided direct evidence that a broad, relatively weak feature of the CD spectrum around 780 nm belongs to the upper exciton component of B850 BChls.[94] We point out that strictly speaking the "upper exciton component" is not really any separate component but a high energy edge of the B850 exciton band which has a considerable intensity (see Figure 5.).

Thus, it appears that there are two qualitatively different contributions to the spectral overlap governing B800 to B850 transfer. First, there is a "normal" overlap mediated by phonons and vibrations; second, there is a direct transfer to the upper edge of B850 exciton band positioned somewhat to the blue of B800. In this picture the temperature dependence of the transfer in different species has different origin. In wild type *Rb. sphaeroides*, the energy gap between the donor and acceptor is substantially larger than *kT*, which implies that the vibronic part of the spectral overlap does not change with lowering temperature. At the same time, the overlap with the 780 nm upper excitonic component is reduced because of the narrowing of the B800 spectrum. In addition, at low temperature fast transfer among inhomogeneously distributed B800 molecules localizes the excitation on the red part of the B800 inhomogeneous distribution (see previous section) which further slows down the upper exciton component induced transfer. At 4 K this transfer channel is probably blocked. If no other transfer channel is present, then the 0.7 and 1.5 ps transfer times at 300 and 4 K in *Rb. sphaeroides* suggest that at room-temperature half of the transfer occurs via the "normal" vibronic band Förster overlap whereas the other half involves the upper exciton level of the B850 band at 780 nm. On the other hand, in the B800−820 of *Rps. acidophila* the upper exciton component should be around 750 nm, which means that it no longer contributes to the B800−B820 spectral overlap even at room temperature. Since the energy gap between the bands is comparable to *kT* at room temperature, the spectral overlap of the phonon sidebands reduces if the temperature is lowered, explaining the observed slow of the transfer from 0.75 ps at 300 K to 0.9 ps at 77 K.[35]

Finally, we note that also higher order super-exchange type coupling mediated by nearby chromophores, particularly carotenoid molecules, has been suggested as an additional possible transfer channel.[27,109] From the crystal structure of LH2 of *Rps. acidophila* it is evident that the carotenoid molecules are within very short distance from both the B800 and B850 BChl *a* molecules. Carotenoid S2 state mediated B800−B850 coupling was recently assessed by Krueger et al.[73] using ab initio calculations. The authors found that the carotenoid S2 state can only lead to a small additional coupling of 2−3 cm^{-1}. At the same time, the authors have found a substantial mixing of the carotenoid and B850 orbitals, which could have a large influence on the B800−B850 coupling. Whether these types of higher order transfer processes are really functional in photosynthetic light harvesting remains to be seen.

7. Energy Transfer within the Strongly Coupled B850 Ring

From the published LH2 structures it is immediately clear that the BChl molecules in the B850 ring are strongly coupled and in fact both calculations and experiments show that the interaction between the BChls within a subunit and between BChls on adjacent subunits is of the order of 300 cm^{-1}.[36,73,78,92,94,131] We note that also much stronger interactions up to 800 cm^{-1} have been suggested.[135,136] It has generally been concluded that not the full redshift can be attributed to excitonic effects and furthermore that not only excitonic effects determine the spectroscopy of LH2. In the following, we will attempt to illustrate this. First, there is a variant of LH2 of *Rps. acidophila* in which the B850 absorption is shifted to 820 nm, whose major structural difference with the B800−850 variant is the H-bonding pattern of the α-BChl.[137,138] The structure of this B800−820 variant is most likely very similar to that of the B800−850 form, resulting in equal excitonic contributions in both complexes. Furthermore, by modulating this H-bonding pattern of the α-BChl in LH2 of *Rb. sphaeroides* the absorption of LH2 could be gradually shifted from 850 to around 820 nm.[7] Secondly, the B850 transition of LH2, similar to the B875 transition of LH1 and the lowest excitonic state of the special pair of the RC, has been shown to exhibit a strong electrochromic response, mainly characterized by a spectacular change in polarizability.[122,139−141] The cause of this large Stark effect is most likely the mixing of an intradimer α-BChl β-BChl charge transfer state with the excited state of the dimer/ring.[139,142,143] Similar to the special pair P,[144] this mixing of CT states with the excited states of the ring may induce a significant red shift of the lowest excitonic states.[142] It might be argued that this effect underlies the further redshift of the LH1 ring to 875 nm,

since for LH1 the observed change in polarizability is even more dramatic than for LH2,[122,140] but this remains to be proven. Third, there is now extensive evidence that the absorption bands of LH2 and LH1 are strongly inhomogeneously broadened,[26,145−148] and nonlinear spectroscopic experiments have shown that this is also true at room temperature.[78,129,149−151] Estimates in these papers for the amount of disorder range between 250 and 500 cm^{-1}, and these values are generally larger than the amount of excitonic coupling. Finally, electron−phonon/vibration coupling, which would be responsible for a dynamic localization of the excitation is estimated to be in the few hundred cm^{-1} range.[152,153]

Since the mid 1980s, a multitude of time-resolved absorption, fluorescence, and more recently, nonlinear, spectroscopic experiments were performed on LH2, LH1, and more intact systems (see for reviews of the earlier work[1−4]). The general conclusion was that, within a picosecond after excitation, the energy transfer was more or less complete, requiring average single site lifetimes of a few hundred femtoseconds at most. In subsequent experiments aimed to time-resolve the B850 and B875 intraband dynamics, fast isotropic kinetics were measured within the B850/B875 band, exploiting the equilibration among an inhomogeneous spectral distribution of pigments exhibiting ultrafast energy transfer.[78,153] Alternatively, the polarized spontaneous emission was measured by fluorescence upconversion[131,150] or by polarized pump−probe experiments.[60,78,153] Recently, three-pulse stimulated photon echoes were obtained that measure the correlation function M(t) of the transition frequency that was originally excited and thus directly reflect all intraband spectral dynamics, including energy transfer.[151,152]

The dynamic red-shift experiments[60,153] were interpreted in terms of a fast (<50 fs) dynamic Stokes' shift followed by a 100−400 fs phase, often bi- or more exponential, that reflected the redistribution of excitation energy over the nonequivalent energetic sites due to energy transfer. Modeling the process as a sequence of hopping events of a localized excitation resulted in single site lifetimes of less than 100 fs, or nearest neighbor energy transfer rates of 100−200 fs.[60,149] The fluorescence depolarization experiments resulted in a major 50 fs component plus a weak slower phase for LH2;[131] for LH1 the depolarization occurred with a major decay time of about 100 fs and a slower phase of about 400 fs.[150] Applying a model that assumed dimer-to-dimer hopping resulted in single site lifetimes of 100 and 80 fs for LH2 and LH1, respectively (note that the faster anisotropy decay in LH2 is mainly a result of the larger depolarization per step in a nonamer, as compared to a 16-mer).

The room-temperature polarized pump−probe experiments on LH1 and LH2 by Chachisvilis et al.[78,154] resulted in similar fast anisotropy decay times: for LH1, about 100 fs in the major absorption band and about 200 fs in the stimulated emission region and for LH2, 60 fs in the major absorption band and about 200 fs in the stimulated emission region. In an attempt to reconcile the isotropic and anisotropic decay times measured in LH2, the same group concluded that a monomer-to-monomer hopping process was not consistent with the results and on the basis of this the authors suggested that the elementary excitation in LH1 and LH2 had a more collective nature. A very similar conclusion was drawn by Monshouwer et al. from isotropic and anisotropic decay experiments on LH1 of *Rps. viridis*.[60] We note that the dimer-to-dimer hopping model introduced by Visser et al.[149] and used later to explain the fluorescence depolarization is consistent with this idea.

Upon lowering the temperature, the inhomogeneous nature of the absorption band was strongly enhanced, resulting in multiexponential and wavelength-dependent kinetics with phases ranging from the 100 fs region to the many picosecond time domain,[78,155] in qualitative agreement with theoretical predictions.[156] The experiments by Chachisvilis et al.[78] at cryogenic temperatures showed that excitation in the blue wing of the B850/B875 absorption still resulted in ultrafast downhill energy transfer. A very similar fast downhill energy transfer at 4 K was observed for *Heliobacterium chlorum*[157] and *Rps viridis* LH1.[60] The model developed for the spectral dynamics due to hopping energy transfer to some extent predicted the observed temperature dependence,[155] assuming a model for the spectral properties of a single site as a function of temperature.[158] However, a close comparison of the isotropic and anisotropic kinetics measured at 4K through the band resulted in a similar discrepancy as mentioned above at room temperature[78] and again led to the conclusion that the elementary excitation in LH1 and LH2 is not localized on a monomer.

At low temperature, a new dynamic feature was observed in LH2 at longer delays by Chachisvilis et al.[78] The stimulated emission/bleaching band broadens and splits into two bands in about 3 ps. The new band is located at about 870 nm and it continues to move further to the red and broadens on the tens of picoseconds time scale. Early 4.2 K steady-state fluorescence measurements of a LH1-less mutant of *Rb. sphaeroides* showed an unusually large Stokes' shift,[159] which was explained as an emission from a minor long-wavelength component of B850. On the other hand, recent time-resolved data were interpreted as a stimulated emission from the lowest exciton component of a disordered ring of B850,[91,160] whereas the slower phases of the dynamics were assigned to the transfer among inhomogeneously distributed rings.[160] The zero phonon hole action spectra have also been interpreted as indication that the lowest exciton component of B850 lies at 870 nm.[33] It is interesting to note that recent Stark hole burning measurements[141] have found a very small dipole moment change for this low exciton band. At the same time the polarizability change in B850 is rather large,[122] leaving open the possibility to explain the slowly relaxing red emission as a polaron formation. The fact that the effect is much less pronounced in LH1 suggests that it may be related to the tendency of LH2 to form very large aggregates[161,162] or to some LH2-specific impurity.

Recently, 3-pulse photon echo peak shift (3PPEPS) experiments were performed for LH1 and LH2[152] and the LH1 subunit B820.[151] The conclusion form this work was that on a time scale of less than 50 fs, due to fast fluctuations in the protein environment, the excitation becomes localized on a small part of the ring, possibly an $\alpha\beta$-$BChl_2$-heterodimer. A similar conclusion was drawn from the ultrafast Stokes' shift in a few tens of femtoseconds (see above).[153,163] In the peak shift decay, which is a direct measure of the transition frequency correlation function, this initial phase was followed both in LH1 and LH2 by an exponential phase that was interpreted as a loss of rephasing capability of the system due to energy transfer. During the energy transfer, the system samples all the possible environments that contribute to the inhomogeneous broadening, and as a consequence, the information about the original environment is lost. The model that assumes hopping on an inhomogeneously broadened ring of dimers gave a qualitative fit to the results. For both light-harvesting complexes the homogeneous broadening was estimated to be 200 cm^{-1}, the inhomogeneous broadening 500 cm^{-1}, and the hopping time about 100 fs. This interpretation was supported by a 3PPEPS experiment on the LH1 subunit, B820, in which the 100 fs phase in the decay of the peakshift ascribed to energy transfer was no

longer present and replaced by a nondecaying component arising from inhomogeneous broadening.[151] The striking similarity between the 3PPEPS of LH1 and B820, apart from the energy transfer phase suggests that in LH1 the elementary excitations are delocalized over small units, possibly dimers.

To quantitatively assess the size of the exciton one can use a variety of experimental approaches. One possibility is is based on the idea that the nonlinear optical properties of aggregates are sensitive to the delocalization length of the electronically excited states. For example, in a linear aggregate of two-level molecules one can calculate the exciton delocalization length from the approximate expression $\Delta\omega \approx 3\pi^2 V/(N+1)^2$, where $\Delta\omega$ is the difference between pump−pulse-induced bleach (ground state to one-exciton transition) and pump−pulse-induced absorption (one-exciton to two-exciton transition) maxima, V is the dipole−dipole interaction between nearest neighbors, and N is the exciton delocalization length.[164] However, monomeric BChl *a* has a strong excited-state absorption in the region of the Q_y transition[165] and therefore B850 is much more realistically described as an aggregate of multilevel (not two-level) molecules where the one- to two-exciton transition has a significant intramolecular component where two photons double excite a single molecule.

Simulations based on the model which includes monomeric doubly excited states and also accounts for the circular organization of the bacteriochlorophyll molecules of B850 suggested that the thermalized delocalization length (2 ps after excitation of B800) of the B850 exciton is 4 ± 2 BChl molecules,[154] the relatively large error limits allowing for the uncertainties in the dipole strength of the monomeric excited-state absorption. In subsequent more detailed calculations, to fit experimental data of LH2 in the temperature range 296−4 K, spectral inhomogeneity of the BChl molecules was also included.[78] It was found that the quantitative value for the delocalization length depends significantly on the definition used. In this work the exciton delocalization length was defined as the fwhm of the ensemble averaged autocorrelation function of the lowest exciton state. It was found that the exciton is delocalized over four BChl *a* molecules of LH2 at ∼1 ps after the excitation (see Figure 9).[78] A recent calculation of the 1 ps room temperature and 77K pump−probe spectra measured for *Rps. viridis* resulted in a very similar estimate.[166]

A second measure that has been considered is the amount of photobleaching of the major transition[167] or the amount of induced absorption per absorbed photon and surprisingly high numbers have been reported for the amplitude of the B850/B875 bleaching following excitation[168−170] or the amount of induced absorption;[187] these effects have generally been interpreted as arising from totally delocalized excitons. However, due to a multitude of effects, singlet−singlet and singlet triplet annihilation among them, these experiments have also been shown to be very sensitive to badly defined experimental conditions. Recently, Monshouwer and co-workers[171] attempted to measure quantitatively the amount of B850 bleaching per absorbed photon relative to the amount of bleaching in the LH1 dimeric subunit B820 and from this experiment it was concluded that the observed bleaching in LH2 corresponded with that expected for an excitation delocalized over about 4 BChls, a result very similar to the earlier B850 absorption difference line shape analyses[78,154] and to that obtained from simultaneously fitting the shape of the pump−probe spectra of B820 and B850.[172]

As was already discussed above, a third measure of the delocalization length is given by the so-called superradiance,

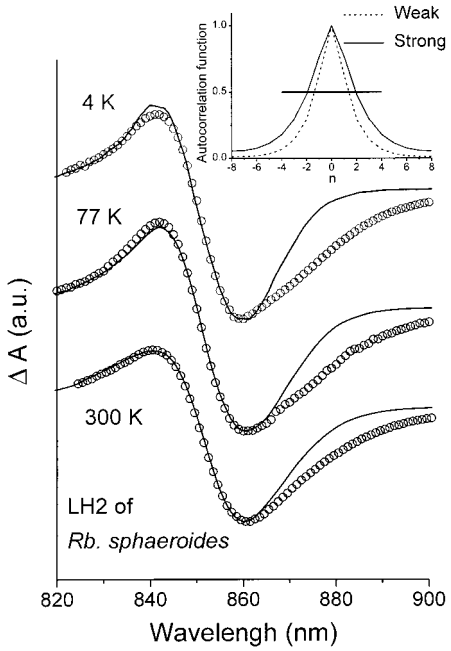

Figure 9. Experimental (circles) and calculated (lines) transient absorption spectra of LH2 at three different temperatures. Experimental spectra are recorded 1.5 ps after excitation at 800 nm. Calculations are carried out with weak interaction ($V = 200$ cm^{-1}), fwhm of the inhomogeneous distribution is 550 cm^{-1}, and homogeneous widths are 25, 50, and 75 cm^{-1} for 4, 77, and 300 K, respectively. In the inset, we present the autocorrelation function (eq 11) of the lowest state of B850 corresponding to the fits in case of strong ($V = 450$ cm^{-1}, solid) and weak ($V = 200$ cm^{-1}, dashed) interaction. (Taken from ref 78.)

or better the radiative rate of LH2. At room temperature, the emitting dipole strength is about 2−3 times that of monomeric BChl *a*, and for LH2 is almost independent of temperature down to 4 K. It was demonstrated above that a calculation of the superradiance as a function of temperature reproduces these experimental observations if significant energetic disorder is assumed.[154] These experiments suggest a coherence length of a few BChl *a* as measured by the fwhm of the averaged exciton wave function and this corresponds nicely to the outcome of the pump−probe results discussed above. For LH1 at room temperature, the superradiance is very similar to that of B850, but upon lowering the temperature the emitting dipole strength increases suggesting that for LH1 disorder plays a somewhat less dominant role than for LH2.

Finally, for several systems including LH2 of *Rb. sphaeroides*,[58,152] LH1 of *Rb. sphaeroides*,[58,150,152,153] LH1 of *R. rubrum*,[59] LH1 of *Rps. viridis*[60] and B820[151,153,163] low-frequency oscillatory phenomena have been observed in transient spectroscopic experiments following excitation with short (<100 fs) pulses. In general these have been attributed to coherent nuclear motion in the excited state, possibly in combination with ground state wave packet motion. The most surprising observation is that these nuclear coherences survive for several picoseconds, a time window in which many energy transfer steps have taken place and the excitation has spectrally "equilibrated". So far there is not a good model to explain this. Nevertheless, it may be clear that these observations are very difficult to reconcile with the traditional Förster model for energy transfer.

8. PSU−Energy Transfer over the Antenna Network and Trapping by the Reaction Center

As illustrated in Figure 10, the LH2 peripheral antenna complex is just one part of the complete photosynthetic unit

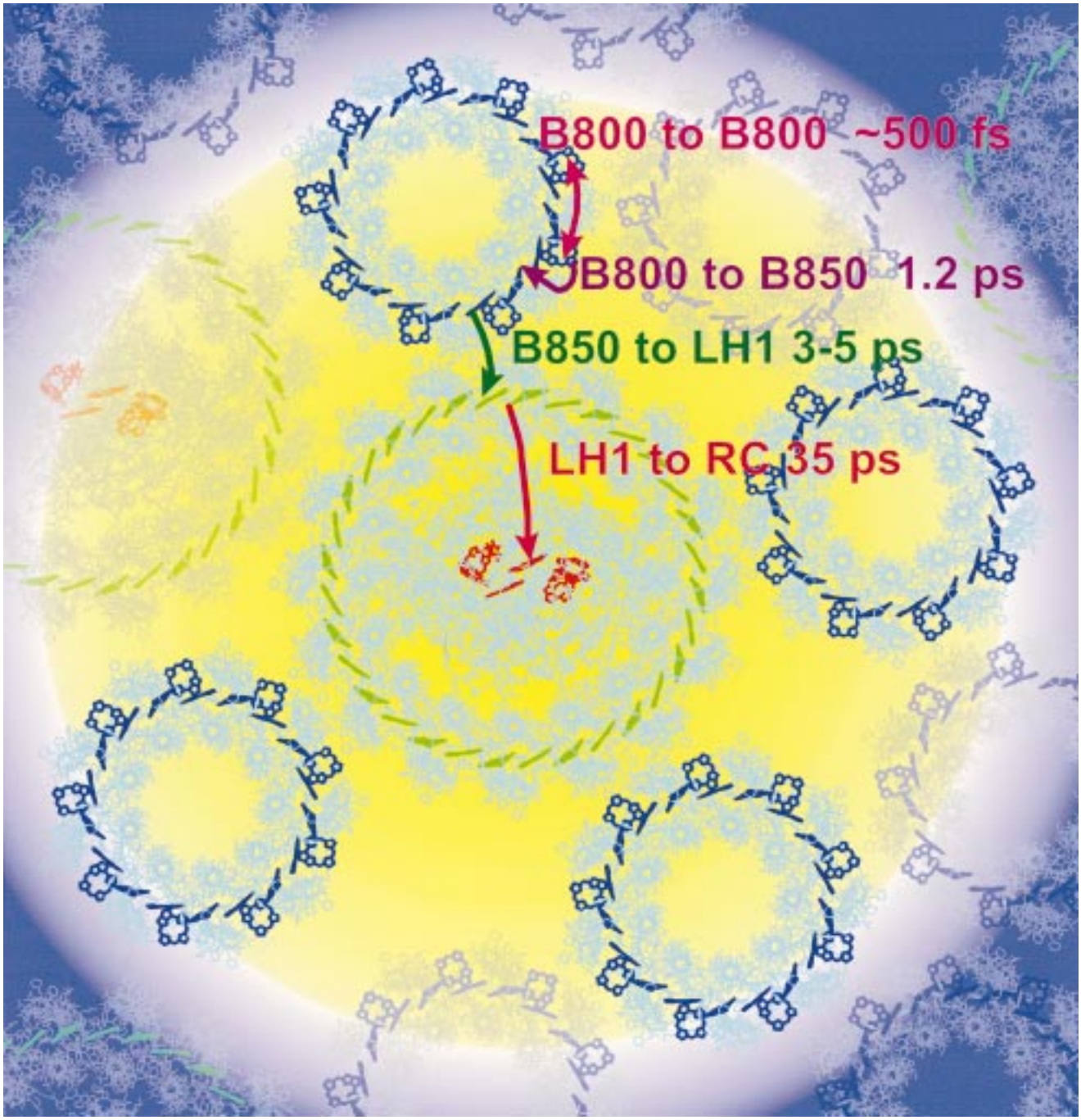

Figure 10. Model of the primary photosynthetic machinery of purple bacteria based on the known structural data. The BChl molecules of LH2 (B800 and B850), LH1 and RC are blue, green and red, respectively. Polypeptides are light blue. The highlighted five rings (four LH2s and one LH1+RC) correspond to a PSU which in this ratio satisfies the approximate 1:2:1 ratio of B800:B850:B875 band intensities in *Rb. sphaeroides*. The boarders of PSUs are tentative and excitation transfer occurs between different PSUs which all together form large domains. The time constants correspond to the kinetics at 77 K. The diameter of the yellow background ring is about 230 Å.

(PSU), the minimal pigment−protein unit capable of performing the primary photosynthetic processes. We will briefly describe the function of LH2 within this unit and we will also show how the different protein complexes cooperate to catch and transfer energy to the reaction center. The first step in moving the energy toward the reaction center, after it has been absorbed by the LH2 complex, is a transfer to another LH2 (B850) or LH1 ring. Experimentally it is difficult to directly study LH2 ring-to-ring transfer (at least at ambient temperatures) since there are no (or very small) spectral changes associated with this process (all LH2 rings are virtually identical). Time-resolved absorption and fluorescence anisotropy are not useful either, because the excitations are already depolarized (within the plane) through the rapid motion inside one ring and very little further depolarization occurs as a result of the ring-to-ring migration. However, LH2 → LH1 ring transfer is easily observable as a result of the differing absorption and fluorescence spectra of the two complexes. Since we do not expect the distances between LH2 rings and between LH2 and LH1 rings to be much different, and since the donor−acceptor spectral overlaps for B850 → B850 and B850 → LH1 energy transfer are quite similar (at least at room temperature when the spectra are broad), we can approximate all ring-to-ring transfer processes with that for LH2 (B850) → LH1.

The first results for this process appeared from absorption and fluorescence measurements with picosecond time resolution

on several different species.[2,21,173−176] Due to the limited time resolution of these experiments and complex kinetics in intact pigment systems, the process was not clearly resolved in most cases. Nevertheless, these early results suggested that the LH2 → LH1 transfer step occurs on the time scale of 5−40 ps. In a femtosecond two-color absorption measurement[39] direct information was obtained on the LH2 → LH1 transfer step. The build-up of LH1 excitations in *Rb. sphaeroides* at room temperature and 77 K was measured following excitation of B800, and the B850 → LH1 transfer step was found to occur with a time constant of ∼3 ps at room temperature and ∼5 ps at 77 K. From femtosecond transient absorption experiments similar to those of Hess et al.,[39] Nagarajan and Parson[40] also concluded that LH2 → LH1 ring-to-ring transfer occurs with a ∼5 ps time constant, and in addition they observed a slower phase (∼25 ps) in the LH2 → LH1 process, which they ascribed to energy migration within the LH2 pool prior to transfer to LH1. Employing an effective Hamiltonian approach to calculate energy transfer rates between the light-harvesting complexes of a PSU modeled on the basis of the *Rs. molischianum* LH2 structure, Hu et al.[177] concluded that LH2 → LH2 and LH2 → LH1 ring-to-ring transfer occurs with the times ∼7 and ∼3 ps, respectively, in good agreement with the experimental results.

How the light-harvesting antenna makes contact with the reaction center and how energy is transferred into the reaction center (trapped) is an important aspect of the function of the whole photosynthetic unit. The early efforts to study the trapping process and work up to approximately 1993 was summarized by Freiberg.[178] Information about this can be obtained by measuring the rate of energy transfer from LH1 to the special pair (P) electron donor in the reaction center, and from it estimating the distance between the LH1 molecules and the special pair. The description of the LH1 excited state is of crucial importance for the result; whether the excitation energy is delocalized over the whole LH1 ring or localized to only a few BChl molecules will obviously be important for interpreting the measurements. A transfer time of ∼35 ps was obtained for this process by measuring the decay of LH1 excitations in the temperature range 77−177 K.[43,179] A similar result was obtained by Beekman et al.[180] by measuring the overall trapping time for a series of RC-mutants of *Rb. sphaeroides*, having modified charge separation times. Freiberg et al.[181] also studied the energy trapping in a series of *Rb. sphaeroides* RC-mutants with slow charge separation and similarly concluded that the LH1 → RC energy transfer is slow compared to all other energy transfer steps in the antenna. Their measurements yielded somewhat longer antenna lifetimes than observed by Beekman et al.,[180] but this did not change the overall conclusion that the LH1 → RC energy transfer is the slowest process in the overall trapping. From a measurement of core antenna fluorescence upon selective RC-excitation, Otte et al.[182] arrived at a similar conclusion. All these results show that energy hopping from one ring to another within the PSU is fast as compared to the total ∼60 ps lifetime of the excitations in the antenna[2,17,170] and the LH1 → RC energy transfer step.[43,170,179−182] This implies that energy transfer from the LH1 antenna to the special pair is the rate-limiting step of the overall energy trapping process. The trapping of excitation energy by photosynthetic reaction centers has often been discussed in terms of the "trap-limited" or "diffusion-limited" model, and consequently, we have termed this new situation "transfer-to-trap-limited" excitation dynamics.[44,75,156,180,183,184]

From the model of the PSU (Figure 10), it appears that this slow rate of LH1 → RC energy transfer is a direct consequence of the size of the reaction center protein, which prevents a shorter antenna special pair distance. It is interesting to speculate about whether this long LH1−P distance is of any functional importance. A trivial reason is that the distance is just determined by the physical size of the RC proteins, i.e., by the size of the RC required to fulfill its function. Another, more interesting reason to have a large distance between the LH1 BChls and the special pair of the reaction center could be that the oxidized primary donor (P^+) is a very reactive species. With a too small LH1−P distance, the antenna BChls could be oxidized by P^+, which would lead to very efficient quenching of the excitation energy within the LH1 antenna. This idea has previously been suggested for the RC of photosystem 2 of green plants for which the oxidized primary donor $P680^+$ has an extremely oxidizing potential. Hence, whatever is the reason for the long LH1−P distance, the organism is thus faced with the problem of keeping the LH1−P distance large enough, but at the same time maximize the LH1 → P energy transfer rate in order to optimize trapping efficiency. The circular arrangement of the LH1-core antenna, where all the antenna pigments can transfer energy to the special pair of the RC with approximately the same rate is obviously one means to increase LH1 → P transfer efficiency. If, for instance, there would only be 4−6 entries into the RC from the LH1 antenna (as was often suggested in the lattice models[185] used before the advent of the crystal structures of LH2 and LH1), the LH1 → P transfer would be many times slower and the trapping efficiency markedly lower than the observed ∼95%. In addition, we conjecture that the exciton delocalization discussed in Sections 3 and 7 is another part of this optimization. It can be estimated that for a LH1 exciton of delocalization length of ∼4 BChl monomer units, the coupling to the special pair will be approximately 4-fold the coupling between a monomeric BChl and P. A 4-fold longer trapping time (i.e. 200−250 ps) would decrease the overall trapping efficiency from the observed ∼95%−∼80%. Interaction between the LH1 exciton states and the special pair of the reaction center has also been discussed by other authors.[186,187] These two factors taken together may therefore increase the trapping rate by as much as a factor of 10, as compared with the situation of a core antenna consisting of weakly coupled pigments having only a few entries into the RC. Thus we propose that the ring-like organization of the LH1 core antenna and its strongly coupled BChl molecules, with the centrally positioned reaction center, is essential for the high trapping efficiency in these organisms.

Acknowledgment. We would like to thank our co-workers of the Department of Chemical Physics, Lund University and Department of Physics and Astronomy, Free University of Amsterdam. We thank Dr. J. L. Herek and Dr. O. Kühn for valuable discussions and critical reading of the manuscript. This work was partly financed by European Union. T.P and V.S. acknowledge support from the Swedish NFR and the K. & A. Wallenberg Foundation.

References and Notes

(1) van Grondelle R. *Biochim. Biophys. Acta* **1985**, *811*, 147.

(2) van Grondelle, R.; Dekker: J. P.; Gillbro, T.; Sundström V. *Biochim. Biophys. Acta* **1994**, *1187*, 1.

(3) Pullerits, T.; Sundström, V. *Acc. Chem. Res.* **1996**, *29*, 381.

(4) Fleming, G. R.; van Grondelle, R. *Curr. Opin. Struct. Biol.* **1997**, *7*, 738.

(5) Duysens, L. N. M. Doctoral Thesis, State University of Utrecht, The Netherlands, 1953.

(6) Miller, K. R. *Nature* **1982**, *300*, 53.

(7) Fowler, G. J. S.; Visschers, R. W.; Grief G. G.; van Grondelle R.; Hunter C. N. *Nature* **1992**, *355*, 848.
(8) Olsen, J. D.; Sockalingum, G. D.; Robert, B.; Hunter, C. N. *Proc. Natl. Acad. Sci. U.S.A.* **1994**, *91*, 7124.
(9) Zuber, H.; Cogdell, R. J. In *Anoxygenic Photosynthetic Bacteria*; Blankenship, R. E., Madigan, M. T., Bauer, C. E., Eds.; Kluwer Academic Publishers: Dordrecht, 1995; p 315.
(10) Hunter, C. N. In *Anoxygenic Photosynthetic Bacteria*; Blankenship, R. E., Madigan, M. T., Bauer, C. E., Eds.; Kluwer Academic Publishers: Dordrecht, 1995; p 473.
(11) Deisenhofer, J.; Epp, O.; Miki, K.; Huber, R.; Michel, H. *Nature* **1985**, *318*, 618.
(12) Zuber, H.; Brunisholz, R. A. In *The Chlorophylls*; Scheer, H., Ed.; CRC Press: Boca Raton, 1993; p 627.
(13) Kramer, H. J. M.; van Grondelle, R.; Hunter, C. N.; Westerhuis, W. H. J.; Amesz, J. *Biochim. Biophys. Acta* **1984**, *765*, 156.
(14) van der Laan, H.; De Caro, C.; Schmidt, Th.; Visschers, R. W.; van Grondelle, R.; Fowler, G. J. S.; Hunter, C. N.; Völker S. *Chem. Phys. Lett.* **1993**, *212*, 569.
(15) Cogdell, R. J.; Frank, H. A. *Biochim. Biophys. Acta* **1987**, *895*, 63.
(16) Bakker, J. G. C.; van Grondelle, R.; den Hollander, W. T. F. *Biochim. Biophys. Acta* **1983**, *725*, 508.
(17) Borisov, A. Yu.; Freiberg, A. M.; Godik, V. I.; Rebane, K. K.; Timpmann, K. K. *Biochim. Biophys. Acta*. **1985**, *807*, 221.
(18) Sundström, V.; van Grondelle, R.; Bergström, H.; Åkesson, E.; Gillbro, T. *Biochim. Biophys. Acta* **1986**, *851*, 431.
(19) Van Grondelle, R.; Bergström, H.; Sundström, V.; Gillbro, T. *Biochim. Biophys. Acta* **1987**, *894*, 313.
(20) Bergström, H.; van Grondelle, R.; Sundström V. *FEBS Lett.* **1989**, *250*, 503.
(21) Freiberg A., Godik V. I., Pullerits T.; Timpmann K. *Biochim. Biophys. Acta* **1989**, *973*, 93.
(22) Shreve, A. P.; Trautman, J. K.; Frank, H. A.; Owens, T. G.; Albrecht, A. C. *Biochim. Biophys. Acta*, **1991**, *1058*, 280.
(23) Hess, S.; Feldchtein, F.; Babin, A.; Nurgaleev, I.; Pullerits, T.; Sergeev, A.; Sundström, V. *Chem. Phys. Lett.* **1993**, *216*, 247.
(24) Monshouwer, R.; Ortiz de Zarate, I.; van Mourik, F.; van Grondelle, R. *Chem. Phys. Lett.* **1995**, *246*, 341.
(25) Van der Laan, H.; Schmidt, Th.; Visschers, R. W.; Visscher, K. J.; van Grondelle, R.; Völker S. *Chem. Phys. Lett*. **1990**, *170*, 231.
(26) Reddy, N. R. S.; Small, G. J.; Seibert, M.; Picorel, R. *Chem. Phys. Lett.* **1991**, *181*, 391.
(27) Pullerits, T.; Hess, S.; Herek, J. L.; Sundström V. *J. Phys. Chem.* **1997**, *101*, 10560.
(28) De Caro, C.; Visschers, R. W.; van Grondelle, R.; Völker, S. *J. Phys. Chem*. **1994**, *98*, 10584.
(29) Van Mourik, F.; Hawthornthwaite, A. M.; Vonk, C.; Evans, M. B.; Cogdell, R. J.; Sundström, V.; van Grondelle, R. *Biochim. Biophys. Acta* **1992**, *1140*, 85.
(30) Monshouwer, R.; Ortiz de Zarate, I.; van Mourik, F.; Picorel, R.; Cogdell, R. J.; van Grondelle, R. In *Photosynthesis: from Light to Biosphere*; Mathis, P., Ed.; Kluwer Academic Publishers: Dordrecht, 1995; Vol. I, p 91.
(31) Wu, H. M.; Cogdell, R. J.; Muenke, H.; Small, G. J. *Mol. Cryst. Liq. Cryst.* **1996**, *291*, 163.
(32) Wu, H.-M.; Savikhin, S.; Reddy, N. R. S.; Jankowiak, R.; Cogdell, R. J.; Struve, W. S.; Small, G. J. *J. Phys. Chem.* **1996**, *100*, 12022.
(33) Wu, H.-M.; Rätsep, M.; Jankowiak, R.; Cogdell, R. J.; Small, G. J. *J. Phys. Chem. B* **1997**, *101*, 7641.
(34) Ma, Y.-Z.; Cogdell, R. J.; Gillbro, T. *J. Phys. Chem. B* **1997**, *101*, 1087.
(35) Ma, Y.-Z.; Cogdell, R. J.; Gillbro, T. *J. Phys. Chem. B* **1998**, *102*, 881.
(36) Monshouwer, R.; van Grondelle, R. *Biochim. Biophys. Acta* **1996**, *1275*, 70−75.
(37) Wendling, M.; Salverda, J. M.; van Mourik, F.; van Grondelle, R. Manuscript in preparation.
(38) Zhang F. G., van Grondelle R.; Sundström V. *Biophys. J.* **1992**, *61*, 911.
(39) Hess, S.; Chachisvilis, M.; Timpmann, K.; Jones, M. R.; Hunter, C. N.; Sundström, V. *Proc. Natl. Acad. Sci. U.S.A.* **1995**, *92*, 12333.
(40) Nagarajan, V.; Parson, W. W. *Biochemistry* **1997**, *36*, 2300.
(41) Sebban, P.; Moya, I. *Biochim. Biophys. Acta* **1983**, *722*, 436.
(42) Freiberg, A.; Godik, V. I.; Timpmann, K. In *Advances in Photosynthesis Research;* Sybesma, C., Ed.; Martinus Nijhoff/Dr W. Junk Publishers: The Hague, 1984; Vol. I, p 45.
(43) Visscher, K. J.; Bergström, H.; Sundström, V.; Hunter, C. N.; van Grondelle, R. *Photosynth. Res.* **1989**, *22*, 211.
(44) Timpmann, K.; Zhang, F. G.; Freiberg, A.; Sundström, V. *Biochim. Biophys. Acta* **1993**, *1183*, 185.
(45) McDermott, G.; Prince, S. M.; Freer, A. A.; Hawthornthwaite-Lawless, A. M.; Papiz, M. Z.; Cogdell, R. J.; Isaacs, N. W. *Nature* **1995**, *374*, 517.
(46) Koepke, J.; Hu, X.; Muenke, C.; Schulten, K.; Michel, H. *Structure* **1996**, *4*, 581.
(47) Karrasch, S.; Bullough, P. A.; Ghosh, R. *EMBO J.* **1995**, *14*, 631−638.
(48) Kleinekofort, W.; Germeroth, L.; van den Broek, J. A.; Schubert, D.; Michel, H. *Biochim. Biophys. Acta* **1992**, *1140*, 102.
(49) Germeroth, L.; Lotspeich, F.; Robert, B.; Michel, H. *Biochemistry* **1993**, *32*, 5615.
(50) Olsen, J. D.; Sturgis, J. N.; Westerhuis, W. H. J.; Fowler, G. J. S.; Hunter, C. N.; Robert, B. *Biochemistry* **1997**, *36*, 12625.
(51) Förster, Th. *Naturwissenschaften* **1946**, *33*, 166.
(52) Robinson, G. W. *Brookhaven Symp. Biol.* **1967**, *19*, 16.
(53) Pearlstein, R. M. *Brookhaven Symp. Biol.* **1967**, *19*, 8.
(54) Shipman, L. L. *Photochem. Photobiol.* **1980**, *31*, 157.
(55) Fetisova, Z. G.; Borisov, A.Yu; Fok, M. V. *J. Theor. Biol.* **1985**, *112*, 41.
(56) Jean, J. M.; Chan, C.-K.; Fleming, G. R.; Owens, T. G. *Biophys. J.* **1989**, *56*, 1203.
(57) Pullerits, T.; Freiberg, A. *Biophys. J.* **1992**, *63*, 879.
(58) Chachisvilis, M.; Pullerits, T.; Jones, M. R.; Hunter, C. N.; Sundström V. *Chem. Phys. Lett.* **1994**, *224*, 345.
(59) Chachisvilis, M.; Fidder, H.; Pullerits, T.; Sundström, V. *J. Raman Spectroscopy* **1995**, *26*, 513.
(60) Monshouwer, R.; Baltuška, A.; van Mourik, F.; van Grondelle, R. *J. Phys. Chem. A.* **1998**, *102*, 4360.
(61) Fenna, R. E.; Matthews, B. W. *Nature* **1975**, *258*, 573.
(62) Davydov, A. S. *Theory of Molecular Excitons;* Plenum: New York, 1971.
(63) Kubo, R.; Toda, M.; Hashitsume, N. *Statistical Physics II: Nonequilibrium Statistical Mechanics;* Springer: Berlin, 1985.
(64) Rahman, T. S.; Knox, R. S.; Kenkre, V. M. *Chem. Phys.* **1979**, *44*, 197.
(65) Kühn, O.; Renger, T.; May, V.; Voigt, J.; Pullerits, T.; Sundström, V. *Trends in Photochem. Photobiol.* **1997**, *4*, 213.
(66) Laible, P. D.; Knox, R. S.; Owens, T. G. *J. Phys. Chem. B* **1998**, *102*, 1641.
(67) Pullerits, T.; van Mourik, F.; Monshouwer, R.; Visschers, R. W.; van Grondelle, R. *J. Lumin.* **1994**, *58*, 168.
(68) Marcus, R. A.; Sutin, N. *Biochim. Biophys. Acta* **1985**, *811*, 265.
(69) Pullerits, T.; Visscher, K. J.; Hess, S.; Sundström, V.; Freiberg, A.; Timpmann, K.; van Grondelle, R. *Biophys. J.* **1994**, *66*, 236.
(70) Monshouwer R., Abrahamsson M., van Mourik F. and van Grondelle R. *J. Phys. Chem. B* **1997**, *101*, 7241.
(71) Dexter, D. L. *J. Chem. Phys.* **1953**, *21*, 836.
(72) Chang, J. C. *J. Chem. Phys.* **1977**, *67*, 3901.
(73) Krueger, B. P.; Scholes, G. D.; Fleming, G. R. *J. Phys. Chem. B* **1998**, *102*, 2284.
(74) Scholes, G. D.; Harcourt, R. D.; Ghiggino, K. P. *J. Chem. Phys.* **1995**, *102*, 9574.
(75) Somsen, O. J. G.; Valkunas, L.; van Grondelle, R. *Biophys. J.* **1996**, *70*, 669.
(76) Meier, T.; Chernyak, V.; Mukamel, S. *J. Phys. Chem.* **1997**, *101*, 7332.
(77) Fidder, H.; Knoester, J.; Wiersma, D. A. *J. Chem. Phys.* **1991**, *95*, 7880.
(78) Chachisvilis, M.; Kühn, O.; Pullerits T.; Sundström V. *J. Phys. Chem. B* **1997**, *101*, 7275.
(79) Kühn, O.; Sundström, V. *J. Chem. Phys.* **1997**, *107*, 4154.
(80) Pullerits, T.; Chachisvilis, M.; Fedchenia, I.; Sundström, V.; Jones, M. R.; Hunter, C. N.; Larsson, S. *Lith. J. Phys.* **1994**, *34*, 329.
(81) Blum, K. *Density Matrix theory and Applications;* Plenum: New York, 1981.
(82) Redfield, A. G.; *Adv. Magn. Reson.* **1965**, *1*, 1.
(83) Jean, J. M. *J. Phys. Chem. A* **1998**, *102*, 7549.
(84) Jean, J. M.; Fleming, G. R. *J. Chem. Phys.* **1995**, *103*, 2092.
(85) Chachisvilis, M.; Sundström, V. *Chem. Phys. Lett.* **1996**, *262*, 165.
(86) Kühn, O.; Sundström, V. *J. Phys. Chem. B* **1997**, *101*, 3432.
(87) Leupold D., Stiel H., Teuchner K., Nowak F., Sandner W., Ücker B.; Scheer H. *Phys. Rev. Lett.* **1996**, *77*, 4675.
(88) Potma, E. O.; Wiersma, D. A. *J. Phys. Chem.* **1998**, *108*, 4894.
(89) Pullerits, T.; Chachisvilis, M.; Sundström, V. In *Photosynthesis: from Light to Biosphere*; Mathis, P., Ed.; Kluwer Academic Publishers: Dordrecht, 1995; Vol. I, p 107.
(90) Leegwater, J. A. *J. Phys. Chem.* **1996**, *100*, 14403.
(91) Kennis, J. T. M.; Streltsov, A. M.; Permentier, H.; Aartsma, T. J.; Amesz, J. *J. Phys. Chem. B* **1997**, *101*, 8369.
(92) Sauer, K.; Cogdell, R. J.; Prince, S. M.; Freer, A. A.; Isaacs, N. W.; Scheer, H. *Photochem. Photobiol*., **1996**, *64*, 564.
(93) Koolhaas, M. H. C.; van der Zwan, G.; Frese, R. N.; van Grondelle, R. *J. Phys. Chem. B.* **1997**, *101*, 7262.

(94) Koolhaas, M. H. C.; Frese, R..N.; Fowler, G. J. S.; Bibby, T. S.; Georgakopoulou, S.; van der Zwan, G.; Hunter, C. N.; van Grondelle, R. *Biochemistry* **1998**, *14*, 4693.
(95) Somsen, O. J. G.; van Grondelle, R.; van Amerongen, H. *Biophys. J.* **1996**, *71*, 1934.
(96) Sieferman-Harms, D. *Physiol. Plant.* **1987**, *69*, 561.
(97) Koyama, Y. *J. Photochem. Photobiol.* **1991**, *9*, 265.
(98) Frank, H. A.; Cogdell, R. J. In *Carotenoids in Photosynthesis*; Young, A., Britton, G., Eds.; Chapman & Hall: London, 1993, p 252.
(99) Frank, H. A.; Christensen, R. L. In *Anoxygenic Photosynthetic Bacteria*; Blankenship, R. E., Madigan, M. T., Bauer, C. E., Eds.; Kluwer Academic Publishers: Amsterdam, 1995; p 373.
(100) Frank, H. A.; Cogdell, R. J. *Photochem. Photobiol.* **1996**, *63*, 257.
(101) Koyama, Y.; Kuki, M.; Andersson, P. O.; Gillbro, T. *Photochem. Photobiol.* **1996**, *63*, 243.
(102) Fleischman, D. E.; Clayton, R. K. *Photochem. Photobiol.* **1968**, *8*, 287.
(103) Holmes, N. G.; Crofts, A. R. *Biochim. Biophys. Acta* **1977**, *459*, 492.
(104) Holmes, N. G.; Hunter, C. N.; Niederman, R. A.; Crofts, A. R. *FEBS Lett.* **1980**, *115*, 43.
(105) Herek, J. L.; Polivka, T.; Pullerits, T.; Fowler, G. J. S.; Hunter, C. N.: Sundström, V. *Biochemistry* **1998**, *37*, 7057.
(106) Freer, A.; Prince, S.; Sauer, K.; Papiz, M.; Hawthornthwaite-Lawless, A.; McDermott, G.; Cogdell, R.; Isaacs, N. W. *Structure* **1996**, *4*, 449.
(107) Shreve, A. P.; Trautman, J. K.; Owens, T. G.; Albrecht, A. C. *Chem. Phys. Lett.* **1991**, *178*, 86.
(108) Nagae, H.; Kikitani, T.; Katoh, T.; Mimuro, M. *J. Chem. Phys.* **1993**, *98*, 8012.
(109) Scholes, G. D.; Harcourt, R. D.; Fleming, G. R. *J. Phys. Chem. B* **1997**, *101*, 7302.
(110) Cogdell, R. J.; Hipkins, M. F.; MacDonald, W.; Truscott, T. G. *Biochim. Biophys. Acta* **1981**, *634*, 191.
(111) Noguchi, T.; Hayashi, H.; Tasumi, T. *Biochim. Biophys. Acta* **1990**, *1017*, 280.
(112) Cogdell, R. J.; Andersson, P. O.; Gillbro, T. *J. Photochem. Photobiol.* **1992**, *15*, 105.
(113) Rademaker, H.; Hoff, A. J.; van Grondelle, R.; Duysens, L. N. M. *Biochim. Biophys. Acta* **1979**, *546*, 248.
(114) Van Grondelle, R.; Kramer, H. J. M.; Rijgersberg, C. P. *Biohim. Biophys. Acta* **1982**, *682*, 208.
(115) Chadwick, B. W.; Zhang, C.; Cogdell, R. J.; Frank, H. A. *Biochim. Biophys. Acta* **1987**, *893*, 444.
(116) Wasielewski, M. R.; Tiede, D. M.; Frank, H. A. In *Ultrafast Phenomena*; Fleming, G. R., Siegman, A. E., Eds.; Springer-Verlag: Berlin, 1986; pp 388−392.
(117) Trautman, J. K.; Shreve, A. P.; Violette, C. A.; Frank, H. A.; Owens, T. G.; Albrecht, A. C. *Proc. Natl. Acad. Sci. U.S.A.* **1990**, *87*, 215.
(118) Andersson, P. O.; Cogdell, R. J.; Gillbro, T. *Chem. Phys.* **1996**, *210*, 195.
(119) Ricci, M.; Bradforth, S. E.; Jimenez, R.; Fleming, G. R. *Chem. Phys. Lett.* **1996**, *259*, 381.
(120) Krueger, B. P.; Scholes, G. D.; Jimenez, R.; Fleming, G. R. *J. Phys. Chem. B* **1998**, *102*, 2284.
(121) Angerhofer, A.; Cogdell, R. J.; Hipkins, M. F. *Biochim. Biophys. Acta* **1986**, *848*, 333.
(122) Beekman, L. M. P.; Frese, R. N.; Fowler, G. J. S.; Picorel, R.; Cogdell, R. J.; van Stokkum, I. H. M.; Hunter, C. N.; van Grondelle, R. *J. Phys. Chem. B.* **1997**, *101*, 7293.
(123) Jackson, J. B.; Crofts, A. R. *FEBS Lett.* **1969**, *4*, 185.
(124) Crielaard, W.; Visschers, R. W.; Fowler, G. J. S.; van Grondelle, R.; Hellingwerf, K. J.; Hunter, C. N. *Biochim. Biophys. Acta* **1994**, *1183*, 473.
(125) Gottfried, D. S.; Steffen, M. A.; Boxer, S. G. *Science* **1991**, *251*, 662.
(126) Hess, S.; Åkesson, E.; Cogdell, R. J.; Pullerits T.; Sundström V. *Biophys. J.* **1995**, *69*, 2211.
(127) Reddy, N. R. S.; Cogdell, R. J.; Zhao, L.; Small, G. J. *Photochem. Photobiol.* **1993**, *57*, 35.
(128) Kennis, J. T. M.; Streltsov, A. M.; Vulto, S. I. E.; Aartsma, T. J.; Nozawa, T.; Amesz, J. *J. Phys. Chem.* **1997**, *101*, 7827.
(129) Joo, T.; Jia, Y.; Yu, J.-Y.; Jonas, D. M.; Fleming, G. R. *J. Phys. Chem.* **1996**, *100*, 2399.
(130) Freiberg, A.; Godik, V. I.; Pullerits, T.; Timpmann, K. *Chem. Phys.* **1988,** *128*, 227.
(131) Jimenez, R.; Dikshit, S. N.; Bradforth, S. E.; Fleming, G. R. *J. Phys. Chem.* **1996**, *100*, 6825.
(132) Hess, S.; Visscher, K. J.; Pullerits, T.; Sundström, V., Fowler, G. J. S.; Hunter, C. N. *Biochemistry* **1994**, *33*, 8300.
(133) Fowler, G. J. S.; Hess, S.; Pullerits, T.; Sundström, V.; Hunter, C. N. *Biochemistry* **1997**, *36*, 11282.
(134) Kolaczkowski, S. V.; Hayes, J. M.; Small, G. J. *J. Phys. Chem.* **1994**, *98*, 13418.
(135) Cory, M. G.; Zerner, M. C.; Hu, X.; Schulten, K. *J. Phys. Chem. B* **1998**, *102*, 7640.
(136) Dracheva, T. V.; Novoderezhkin, V. I.; Razjivin, A. P. *FEBS Lett.* **1996**, *387*, 81.
(137) Fowler, G. J. S.; Sockalingum, G. D.; Robert, B.; Hunter, C. N. *Biochem. J.* **1994**, *299*, 695.
(138) Sturgis, J. N.; Robert, B. *Photosynth. Res.* **1996**, *50*, 5.
(139) Middendorf, T. R.; Mazzola, L. T.; Lao, K.; Steffen, M. A.; Boxer, S. G. *Biochim. Biophys. Acta* **1993**, *1143*, 223.
(140) Beekman, L. M. P.; Steffen, M.; van Stokkum, I. H. M.; Olsen, J. G.; Hunter, C. N.; Boxer, S. G.; van Grondelle, R. *J. Phys. Chem. B* **1997**, *101*, 7284.
(141) Rätsep, M.; We, H.-M.; Hayes, J. M.; Blankenship, R. E.; Cogdell, R.J.; Small, G. J. *J. Phys. Chem. B* **1998**, *102*, 4035.
(142) Alden, R. G.; Johnson, E.; Nagarajan, V.; Parson, W. W.; Law, C. J.; Cogdell, R. G. *J. Phys. Chem. B.* **1997**, *101*, 4667.
(143) Somsen, O. J. G.; Chernyak, V.; Frese, R. H.; van Grondelle, R.; Mukamel, S. *J. Phys. Chem. B* **1998**. In press.
(144) Warshel, A.; Parson, W. W. *J. Am. Chem. Soc.* **1987**, *109*, 6143.
(145) Timpmann, K.; Freiberg, A.; Godik, V. I. *Chem. Phys. Lett.* **1991**, *182*, 617.
(146) Pullerits, T.; Freiberg, A. *Chem. Phys.* **1991**, *149*, 409.
(147) Van Mourik, F.; Visschers, R. W.; van Grondelle, R. *Chem. Phys. Lett.* **1992**, *193*, 1.
(148) Visschers, R. W.; van Mourik, F.; Monshouwer, R.; van Grondelle, R. *Biochim. Biophys. Acta* **1993**, *1141*, 238.
(149) Visser, H. M.; Somsen, O. J. G.; van Mourik, F.; Lin, S.; van Stokkum, I. H. M.; van Grondelle, R. *Biophys. J.* **1995**, *69*, 1083.
(150) Bradforth, S. E.; Jimenez, R.; van Mourik, F.; van Grondelle, R.; Fleming, G. R. *J. Phys. Chem.* **1995**, *99*, 16179.
(151) Yu, J.-Y.; Nagasawa, Y.; van Grondelle, R.; Fleming, G. R. *Chem. Phys. Lett.* **1997**, *280*, 404.
(152) Jimenez, R.; van Mourik, F.; Yu, J.-Y.; Fleming, G. R. *J. Phys. Chem. B.* **1997**, *101*, 7350.
(153) Kumble, R.; Palese, S.; Visschers, R. W.; Dutton, P. L.; Hochstrasser, R. M. *Chem. Phys. Lett.* **1996**, *261*, 396.
(154) Pullerits T., Chachisvilis M.; Sundström V. *J. Phys. Chem*. **1996**, *100*, 10787.
(155) Visser, H. M.; Somsen, O. J. G.; van Mourik, F.; van Grondelle, R. *J. Phys. Chem.* **1996**, *100*, 18859.
(156) Somsen, O. J. G.; van Mourik, F.; van Grondelle, R.; Valkunas, L. *Biophys. J.* **1994**, *66*, 1580.
(157) Liebl, U.; Lambry, J.-L.; Breton, J.; Martin, J.-L.; Vos, M. H. *Biochemistry* **1997**, *36*, 5912.
(158) Pullerits, T.; Monshouwer, R.; van Mourik, F.; van Grondelle, R. *Chem. Phys.* **1995**, *194*, 395.
(159) Van Dorssen, R. J.; Hunter, C. N.; van Grondelle, R.; Korenhof, A. H.; Amesz, J. *Biochim. Biophys. Acta* **1988**, *932*, 179.
(160) Freiberg, A.; Jackson, J. A.; Lin, S.; Woodbury, N. W. *J. Phys. Chem. A* **1998**, *102*, 4372.
(161) Van Grondelle, R.; Hunter, C. N.; Bakker, J. G. C.; Kramer, H. J. M. *Biochim. Biophys. Acta* **1994**, *723*, 30.
(162) Vos, M.; van Dorssen, R. J.; Amesz, J.; van Grondelle, R.; Hunter, C. N. *Biochim. Biophys. Acta* **1988**, *933*, 132.
(163) Diffey, W. M.; Homoelle, B. J.; Edington, M. D.; Beck, W. F. *J. Phys. Chem. B* **1998**, *102*, 2776.
(164) Van Burgel, M.; Wiersma D. A.; Duppen K. *J. Chem. Phys.* **1995**, *102*, 20.
(165) Becker, M.; Nagarajan, V.; Parson, W. W. *J. Am. Chem. Soc.*, **1991**, *113*, 6840.
(166) Novoderezhkin, V. I.; Monshouwer, R.; van Grondelle, R. Manuscript in preparation.
(167) Novoderezhkin, V. I.; Razjivin, A. P. *FEBS Lett.* **1995**, *368*, 370.
(168) Xiao, W.; Lin, S.; Taguchi, A. K. W.; Woodbury, N. W. *Biochemistry* **1994**, *33*, 8312.
(169) Abdourakhmanov, I. A.; Danielius, R.; Razjivin, A. P. *FEBS Lett.* **1989**, *245*, 47.
(170) Kennis, J. T. M.; Aartsma, T. J.; Amesz, J. *Biochim. Biophys. Acta* **1994**, *188*, 278.
(171) Monshouwer, R. Doctoral Theses, Free University of Amsterdam, The Netherlands, 1998.
(172) Novoderezhkin, V. I.; Monshouwer, R.; van Grondelle, R. *J. Phys. Chem. B* **1998** Submitted for publication.
(173) Zhang, F. G.; Gillbro, T.; van Grondelle, R.; Sundström, V. *Biophys. J.* **1992**, *61*, 694.
(174) Müller, M.; Drews, G.; Holzwarth, A. *Biochim. Biophys. Acta* **1993**, *1142*, 49.
(175) Kennis, J. T. M.; Aartsma, T. J.; Amesz, J. *Chem. Phys.* **1995**, *194*, 285.
(176) Kramer, H.; Deinum, G.; Gardiner, A. T.; Cogdell, R. J.; Francke, C.; Aartsma, T. J.; Amesz, J. *Biochim. Biophys. Acta* **1995**, *1231*, 33.

(177) Hu, X.; Ritz, T.; Damjanovic, A.; Schulten, K. *J. Phys. Chem. B* **1997**, *101*, 3854.
(178) Freiberg, A. In *Anoxygenic Photosynthetic Bacteria*; Blankenship, R. E., Madigan, M. T., Bauer, C. E., Eds.; Kluwer Academic Publishers: Dordrecht, 1995; p 385.
(179) Bergström, H.; van Grondelle, R.; Sundström, V. *FEBS Lett.* **1989**, *250*, 503.
(180) Beekman, L. M. P.; van Mourik, F.; Jones, M. R.; Visser, H. M.; Hunter, C. N.; van Grondelle, R. *Biochemistry*, **1994**, *33*, 3143.
(181) Freiberg, A.; Allen, J. P.; Williams, J. A. C.; Woodbury, N. W. *Photosynth. Res.* **1996**, *48*, 309.
(182) Otte, S. C. M.; Kleinherenbrink, F. A. M.; Amesz, J. *Biochim. Biophys. Acta* **1993**, *1143*, 84.
(183) Timpmann, K.; Freiberg, A.; Sundström, V. *Chem. Phys.* **1995**, *194*, 275.
(184) Van Grondelle, R.; Sundström, V. In *The Chlorophylls*; Scheer, H., Ed.; CRC Press: Boca Raton, USA, 1993; p 403.
(185) Pearlstein, R. M. *Photochem. Photobiol.* **1982**, *35*, 835.
(186) Novoderezhkin, V. I.; Razjivin, A. P. *Photosynth. Res.* **1994**, *42*, 9.
(187) Owen, G. M.; Hoff, A. J.; Jones, M. R. *J. Phys. Chem. B* **1997**, *101*, 7197.